J. Fluid Mech. (1974), *vol.* 65, *part* 2, *pp.* 365–400
Printed in Great Britain

Inertial migration of rigid spheres in two-dimensional unidirectional flows

By B. P. HO AND L. G. LEAL
Chemical Engineering, California Institute of Technology, Pasadena

(Received 4 September 1973)

The familiar Segré–Silberberg effect of inertia-induced lateral migration of a neutrally buoyant rigid sphere in a Newtonian fluid is studied theoretically for simple shear flow and for two-dimensional Poiseuille flow. It is shown that the spheres reach a stable lateral equilibrium position independent of the initial position of release. For simple shear flow, this position is midway between the walls, whereas for Poiseuille flow, it is 0·6 of the channel half-width from the centre-line. Particle trajectories are calculated in both cases and compared with available experimental data. Implications for the measurement of the rheological properties of a dilute suspension of spheres are discussed.

1. Introduction

The phenomenon of inertia-induced cross-stream migration of small suspended particles in flowing suspensions has occupied a central position in the rheology and mechanics of such materials since the classical investigations of Segré & Silberberg (1962*a*, *b*, 1963). Though there had been occasional prior reports in the literature of non-uniform concentration distributions of particles in pipe flow (cf. Starkey 1956), these authors provided the first conclusive demonstration that neutrally buoyant rigid spheres in Poiseuille flow could, under appropriate circumstances, migrate across streamlines. More surprising than the existence of migration, however, was Segré & Silberberg's observation that the spheres eventually attained an equilibrium position at approximately 0·6 of the tube radius from the tube centre-line.

Following Segré & Silberberg, many subsequent experimental studies have been reported in which either the bulk flow configuration or the particle properties differed from those of the original work. Many of these are summarized in two excellent review articles, one by Goldsmith & Mason (1966) and the other by Brenner (1966). More recent investigations have been reported by Tachibana (1973) and Halow & Wills (1970*a*, *b*). These various studies show that the general behaviour for rigid *spheres* depends strongly on the specific bulk flow geometry and on whether or not the particle is neutrally buoyant. For Couette flow, neutrally buoyant rigid spheres migrate to the centre-line, while for both two- and three-dimensional Poiseuille flow, the sphere ultimately attains an equilibrium position which is approximately 60% of the way from the centre-line to the vessel walls. On the other hand, a non-neutrally buoyant sphere subjected

to Poiseuille flow through a vertical flow channel is found to migrate towards the walls if its velocity is greater than the undisturbed fluid velocity evaluated at the same point, but towards the centre-line if the particle velocity lags behind the undisturbed fluid velocity.

In the present paper, we consider the case of a neutrally buoyant rigid sphere suspended in a Newtonian fluid which is undergoing either simple shear flow or a two-dimensional Poiseuille flow between two infinite plane boundaries. Many previous investigations have attempted to provide a theoretical description of the migration phenomenon. Experimentally, it has been recognized for some time that a neutrally buoyant rigid sphere suspended in a laminar unidirectional flow will rotate and translate *without* crossing the undisturbed streamlines, provided that the appropriate particle Reynolds number is sufficiently small. Indeed, Bretherton (1962) has shown theoretically that, if the inertia terms of the equations of motion are completely neglected, no lateral force can exist for a body of revolution in a unidirectional flow. Theoretical treatment of the migration problem thus requires inclusion of inertia effects. All investigators to date have used asymptotic expansions for small but non-zero values of the Reynolds number as a means of estimating the inertial contribution to the lateral motion of the particle. The two best known studies are those of Rubinow & Keller (1961) and Saffman (1965). Rubinow & Keller (1961) considered the case of a rigid sphere which is simultaneously spinning with an angular velocity $\boldsymbol{\Omega}_s$ and translating (in a perpendicular direction) at a velocity $\mathbf{U}_s$ through an unbounded stationary fluid at small (but non-zero) Reynolds number. The lateral force resulting in this case is

$$\mathbf{F}_L = \pi a^3 \rho_0 \boldsymbol{\Omega}_s \times \mathbf{U}_s, \tag{1.1}$$

in which ρ_0 is the fluid density and a is the radius of the spherical particle. Saffman (1965) considered the case of a uniform shear flow (with shear rate β^*) of an unbounded fluid of viscosity μ_0. The sphere was assumed to rotate with an angular velocity $\boldsymbol{\Omega}_s$ parallel to the vorticity vector of the undisturbed shear flow, and to translate with a velocity V relative to the local undisturbed velocity of the suspending fluid. The magnitude of the lateral force for this 'slip–shear' case is

$$F_L = 6{\cdot}46 \mu_0 V a^2 (\beta^* \rho_0 / \mu_0)^{\frac{1}{2}}, \tag{1.2}$$

which differs radically from that predicted by the 'slip–spin' mechanism of Rubinow & Keller (1961). In particular, the magnitude of the lateral force given by (1.2) is completely independent of the rate of rotation of the particle. The direction of the force (1.2) is such that a sphere lagging behind the local undisturbed fluid would migrate in the direction of the larger, undisturbed velocity, while a sphere leading the undisturbed flow would migrate in the opposite direction. Although a number of attempts have been made to use the theories of Rubinow & Keller (1961) and of Saffman (1965) to explain or correlate experimental observations of lateral migration, neither furnishes a satisfactory fundamental explanation of the phenomenon for the motion of neutrally buoyant particles in tubes or other bounded flow systems. Cox & Brenner (1968) were the first to consider the complete three-dimensional Poiseuille problem taking

account of the presence of the walls and the non-uniformity of the shear. These authors used the method of matched asymptotic expansions with two small parameters, the Reynolds number and the ratio a/R_0 of the sphere radius to the tube radius, to solve for the inertia-induced force and torque on the sphere. Unfortunately, however, the solution is not given in explicit form, but rather involves a number of very complex integral functions. As a result, no definite conclusions can be reached regarding the direction of the lateral force, its precise magnitude at any given radial position or even the presence or absence of an equilibrium position corresponding to the original observation of Segré & Silberberg.

Two-dimensional Poiseuille flow was previously studied experimentally and theoretically by Repetti & Leonard (1966), who attempted to explain the observed phenomenon of intermediate equilibrium positions by means of the Rubinow–Keller slip–spin theory. Most recently, Tachibana (1973) reported experimental results for two- and three-dimensional Poiseuille flow and concluded that the equilibrium positions are identical for both cases. Couette flow was investigated, both experimentally and theoretically, by Halow & Wills (1970*a*, *b*). The experimental work of these authors included a determination of equilibrium positions, as well as detailed measurements of the particle trajectories, prior to reaching equilibrium. The theory proposed was based upon the solution of Saffman (1965) and was represented as providing agreement with the particle trajectories. However, this agreement must be considered fortuitous since it was only achieved after multiplying Saffman's original (corrected) lift force by an empirical factor of 5. Our present analysis is closely similar to that of Cox & Brenner (1968). Specifically, we use the method of reflexions (equivalent to the formal expansion in a/R_0) to obtain the necessary solutions of the fluid motion. The lateral force on and velocity of the sphere are evaluated from these solutions using the generalized reciprocal theorem of Lorentz. By restricting our attention to two-dimensional flows between plane boundaries, we have been able to evaluate the magnitude and direction of the lateral force. In the next section of the paper, we outline the general method of solution and derive the necessary governing equations. The third section outlines the solution for creeping motion of a sphere suspended in a general quadratic bulk flow between two plane walls when the sphere is located at an arbitrary position between them (though not too close to either wall). The fourth section considers the related problem of the creeping motion of a sphere normal to two parallel walls when the sphere is again located at an arbitrary position between them. In the fifth section, we use these two solutions and the generalized reciprocal theorem to calculate the lateral force on the particle for both the simple shear and two-dimensional Poiseuille flow configurations. Finally, in the last two sections we provide trajectory calculations for a sphere and consider the steady-state concentration distribution for various bulk flow rates in the presence of translational Brownian motion. The trajectory calculations are compared with available experimental data in the Couette and two-dimensional Poiseuille systems. The non-uniform concentration distributions lead to an apparent non-Newtonian viscosity behaviour for two-dimensional Poiseuille flow, the behaviour depending on the

specific apparatus. This result is discussed in light of current theories of suspension rheology and of the related experimental data of Segré & Silberberg (1963) for apparent viscosities in tube flow of a dilute suspension of rigid spheres.

2. The basic equations

We consider a neutrally buoyant rigid sphere of radius a freely suspended in an incompressible Newtonian fluid which is confined between two parallel infinite plane walls separated by a distance d. The suspending fluid is assumed to be undergoing either a simple shear flow or a two-dimensional Poiseuille flow. We denote the fluid viscosity by μ_0 and its density by ρ_0. The basic flow geometry and remaining physical variables for the problem are depicted in figure 1. Of particular importance is d_1, the distance from the stationary wall in shear flow or from the bottom wall in two-dimensional Poiseuille flow to the centre of the particle. Also, as indicated, we employ co-ordinate axes fixed with respect to the particle for the basic analysis, with x^* in the direction of the undisturbed velocity, y^* in the direction of the undisturbed vorticity and z^* in the cross-stream direction. The origin of the co-ordinate system is coincident with the centre of the particle, hence, the walls in this system are located at $z^* = -d_1$ and $z^* = d - d_1$, respectively. We assume that the sphere is translating at a velocity $\mathbf{U}_s^*$ and rotating with an angular velocity $\boldsymbol{\Omega}_s^*$. As we have noted in the introduction, there can be no lateral (z) component to $\mathbf{U}_s^*$ in the absence of inertial effects in the disturbance flow induced by the particle. The prime objective of the present work is the calculation of the first inertia-induced contribution to the z component U_{sz}^*. In the following analysis, all variables will be non-dimensionalized with respect to the characteristic length scale a and an as yet unspecified velocity scale V_c^*. Variables with the superscript * are dimensional and all others non-dimensional, except for the obvious dimensional length scales a, d and d_1. The Reynolds number is then defined as $Re \equiv \rho_0 V_c^* a/\mu_0$.

We begin the detailed analysis with the full dimensionless governing equations and boundary conditions for the velocity and pressure fields $\mathbf{U}$ and P expressed in the particle-fixed co-ordinates indicated previously:

$$\left.\begin{aligned} &\nabla^2\mathbf{U} - \nabla P = Re\,(\mathbf{U}.\nabla\mathbf{U}), \quad \nabla.\mathbf{U} = 0, \\ &\mathbf{U} = \boldsymbol{\Omega}_s \times \mathbf{r} \quad \text{on} \quad r = 1, \\ &\mathbf{U} = \mathbf{V}_w - \mathbf{U}_s \quad \text{on} \quad \text{the walls}, \\ &\mathbf{U} \to \mathbf{V} \quad \text{as} \quad r \to \infty. \end{aligned}\right\} \tag{2.1}$$

Here, $\mathbf{V}$ represents the dimensionless undisturbed bulk flow while $\mathbf{V}_w$ is the dimensionless velocity of the walls. The undisturbed flow $(\mathbf{V}, Q)$ is measured relative to the particle-fixed co-ordinate system described earlier. In order to consider the simple shear and two-dimensional Poiseuille flows simultaneously, the undisturbed velocity and pressure fields will thus be expressed in the general form

$$\mathbf{V} = (\alpha + \beta z + \gamma z^2)\,\mathbf{e}_x - \mathbf{U}_s, \quad Q = 2\gamma x, \tag{2.2}$$

where α, β and γ in simple shear flow are given by

$$\alpha = V_w s, \quad \beta = V_w \kappa, \quad \gamma = 0, \tag{2.3}$$

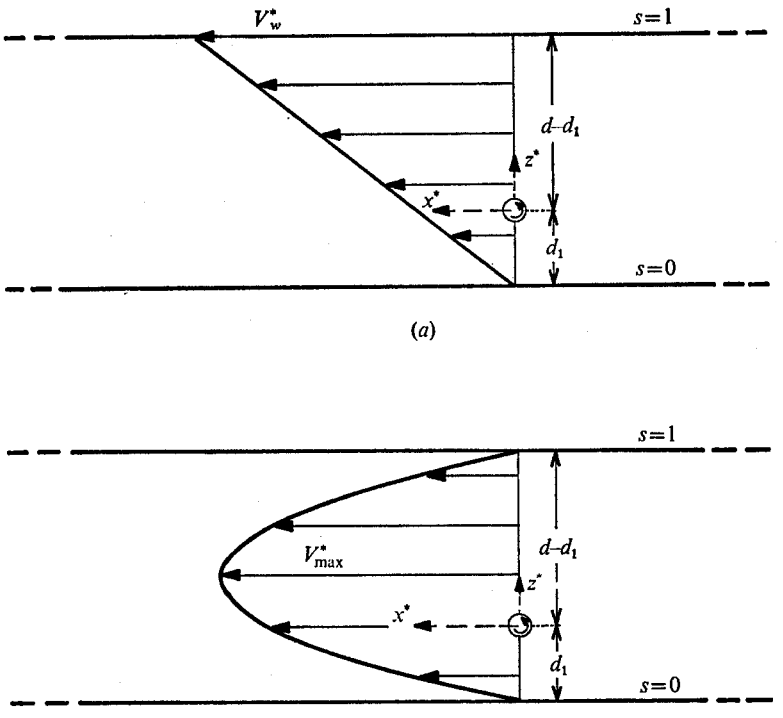

FIGURE 1. The physical system for (*a*) simple shear flow and (*b*) two-dimensional Poiseuille flow.

and in two-dimensional Poiseuille flow take the form

$$\alpha = 4V_{\max} s(1-s), \quad \beta = 4V_{\max}(1-2s)\kappa, \quad \gamma = -4V_{\max}\kappa^2. \tag{2.4}$$

In the above $s = d_1/d$ and $\kappa = a/d$, with d_1 defined in figure 1. Both V_w and $V_{\max}$ are non-dimensionalized with respect to V_c^*.

The solution of (2.1) is aided by introducing the disturbance velocity and pressure fields $\mathbf{v} = \mathbf{U} - \mathbf{V}$ and $q = P - Q$. Since the undisturbed fields $\mathbf{V}$ and Q themselves satisfy the equations and boundary condition

$$\left.\begin{aligned} &\nabla^2\mathbf{V} - \nabla Q = 0, \quad \nabla.\mathbf{V} = 0, \\ &\mathbf{V} = \mathbf{V}_w - \mathbf{U}_s \quad \text{on} \quad \text{the walls} \end{aligned}\right\} \tag{2.5}$$

for all values of the mean (bulk flow) Reynolds number,† it is straightforward to obtain the governing differential equations and boundary conditions for the disturbance fields:

$$\left.\begin{aligned} \nabla^2\mathbf{v} - \nabla q &= Re\,(\mathbf{v}.\nabla\mathbf{v} + \mathbf{v}.\nabla\mathbf{V} + \mathbf{V}.\nabla\mathbf{v}), \\ \nabla.\mathbf{v} &= 0, \\ \mathbf{v} &= \boldsymbol{\Omega}_s \times \mathbf{r} - \mathbf{V} \quad \text{on} \quad r = 1, \\ \mathbf{v} &= 0 \quad \text{on} \quad \text{the walls}, \\ \mathbf{v} &\to 0 \quad \text{as} \quad r \to \infty. \end{aligned}\right\} \tag{2.6}$$

† The inertia terms vanish identically for the unidirectional flows considered here.

In addition, since the disturbance flow is generated by the shear field acting on the sphere, it is clear that the appropriate characteristic velocity V_c^* defining the Reynolds number in (2.1) and (2.6) is the shear velocity $V_w^*(a/d)$ for simple shear flow and $V_{\max}^*(a/d)$ for two-dimensional Poiseuille flow.† Thus, the appropriate Reynolds number for the disturbance flow $(\mathbf{v}, q)$ is $Re \equiv \rho_0 V_w^* \kappa a/\mu_0$ for simple shear flow and $Re \equiv \rho_0 V_{\max}^* \kappa a/\mu_0$ for two-dimensional Poiseuille flow. The present paper is concerned with the solution of (2.6) in the double limit $Re \to 0$ with κ fixed, followed by $\kappa \to 0$. We shall soon see that it is necessary to have $Re \ll \kappa^2$ for the present method of solution. It is also worthwhile to note that the Reynolds number for the bulk flow $(\mathbf{V}, Q)$, say $\overline{Re} \equiv \rho_0 V_w^* d/\mu_0$ for the simple shear flow, is $\overline{Re} = Re\,\kappa^{-2}$. Thus, the condition $Re \ll \kappa^2$ also implies that $\overline{Re} \ll 1$.

Following the approach of Cox & Brenner (1968), we thus proceed by postulating the existence of an asymptotic expansion for $\mathbf{v}$, q, $\mathbf{U}_s$ and $\boldsymbol{\Omega}_s$ of the form

$$\left.\begin{aligned} \mathbf{v} &= \mathbf{v}^{(0)} + Re\,\mathbf{v}^{(1)} + \ldots, \qquad q = q^{(0)} + Re\,q^{(1)} + \ldots, \\ \mathbf{U}_s &= \mathbf{U}_s^{(0)} + Re\,\mathbf{U}_s^{(1)} + \ldots, \quad \boldsymbol{\Omega}_s = \boldsymbol{\Omega}_s^{(0)} + Re\,\boldsymbol{\Omega}_s^{(1)} + \ldots, \end{aligned}\right\} \tag{2.7}$$

in which the individual terms $(\mathbf{v}^{(0)}, q^{(0)})$ and $(\mathbf{v}^{(1)}, q^{(1)})$ satisfy the equations

$$\left.\begin{aligned} &\nabla^2\mathbf{v}^{(0)} - \nabla q^{(0)} = 0, \quad \nabla\cdot\mathbf{v}^{(0)} = 0, \\ &\mathbf{v}^{(0)} = \boldsymbol{\Omega}_s^{(0)} \times \mathbf{r} - (\alpha + \beta z + \gamma z^2)\,\mathbf{e}_x + \mathbf{U}_s^{(0)} \quad \text{on} \quad r = 1, \\ &\mathbf{v}^{(0)} = 0 \quad \text{on} \quad \text{the walls}, \\ &\mathbf{v}^{(0)} \to 0 \quad \text{as} \quad r \to \infty \end{aligned}\right\} \tag{2.8}$$

and

$$\left.\begin{aligned} &\nabla^2\mathbf{v}^{(1)} - \nabla q^{(1)} = \mathbf{v}^{(0)}\cdot\nabla\mathbf{v}^{(0)} + \mathbf{v}^{(0)}\cdot\nabla\mathbf{V} + \mathbf{V}\cdot\nabla\mathbf{v}^{(0)}, \\ &\nabla\cdot\mathbf{v}^{(1)} = 0, \\ &\mathbf{v}^{(1)} = \boldsymbol{\Omega}_s^{(1)} \times \mathbf{r} + \mathbf{U}_s^{(1)} \quad \text{on} \quad r = 1, \\ &\mathbf{v}^{(1)} = 0 \quad \text{on} \quad \text{the walls}, \\ &\mathbf{v}^{(1)} \to 0 \quad \text{as} \quad r \to \infty. \end{aligned}\right\} \tag{2.9}$$

The condition for large r in (2.9) requires justification since it is well known that, to solve the Navier–Stokes equations by perturbation expansion, an outer expansion is generally required and a matching of the inner and outer expansions is necessary to obtain higher-order corrections. In the present case, however, Cox & Brenner (1968) have shown that the first term in the outer expansion is of smaller order than the Reynolds number to the first power, so that 'matching' for $Re\,\mathbf{v}^{(1)}$ is accomplished by simple application of the *natural* boundary condition, namely $\mathbf{v}^{(1)} \to 0$ as $\mathbf{r} \to \infty$. Alternatively, it may be verified from the solution for $(\mathbf{v}^{(0)}, q^{(0)})$ that the ratio of inertia to viscous terms is $Re\,\kappa^{-1}(r^*/a)$. Hence, close to and within the walls $r^* = O(d)$, the Stokes solution, provides a uniformly valid first approximation provided that $Re \ll \kappa^2$. In any case, it is clear that the outer expansion in Re is not required to obtain the lateral velocity to $O(Re)$.

† However, if the sphere is not neutrally buoyant, so that an appreciable slip velocity is introduced, the dominant disturbance may be generated by this slip velocity and the appropriate characteristic velocity for the Reynolds number would be the slip velocity.

The particle satisfies the usual equations of rigid-particle dynamics with no external force and torque. Because of the $O(Re)$ migration, the particle does suffer translational and angular accelerations, but these are $O(Re^2)$. Hence, there is no net hydrodynamic force or torque on the particle at $O(1)$ and $O(Re)$, and this fact is used to calculate $\mathbf{U}_s$ and $\boldsymbol{\Omega}_s$ to $O(Re)$. The zeroth-order terms $\mathbf{U}_s^{(0)}$ and $\boldsymbol{\Omega}_s^{(0)}$ are the translational and angular velocity of the sphere in the absence of inertia and can be written as

$$\mathbf{U}_s^{(0)} = U_{sx}^{(0)}\mathbf{e}_x, \quad \boldsymbol{\Omega}_s^{(0)} = \Omega_{sy}^{(0)}\mathbf{e}_y. \tag{2.10}$$

The first-order correction, taking inertia into account, contributes the additional translational and angular velocities $\mathbf{U}_s^{(1)}$ and $\boldsymbol{\Omega}_s^{(1)}$. At present,we are interested in calculating the lateral migration velocity $U_{sz}^{(1)}$, which is the z component of $\mathbf{U}_s^{(1)}$. Clearly, $U_{sz}^{(1)}$ could be determined by solving for $\mathbf{v}^{(1)}$ leaving $\mathbf{U}_s^{(1)}$ and $\boldsymbol{\Omega}_s^{(1)}$ unspecified and then applying the conditions of zero net external force and torque on the freely suspended particle; however, it can be shown that a complete solution for $\mathbf{v}^{(1)}$ is not necessary for this purpose. Instead, a version of the well-known reciprocal theorem of Lorentz which we shall outline in the next paragraph can be employed; this allows the migration velocity to be expressed in terms of a certain volume integral over the total fluid volume. Careful application of the reciprocal theorem also provides a proof of the fact that the lateral velocity calculated in the manner outlined above produces results identical to those of the approach outlined by Cox & Brenner (1968), in which one, in effect, first calculates the force required to prevent migration.

Suppose that $\boldsymbol{\tau}^{(1)}$ is the stress tensor corresponding to the velocity and pressure fields $\mathbf{v}^{(1)}$ and $q^{(1)}$ and $\mathbf{f}$ is the inhomogeneous part of the governing equation for $(\mathbf{v}^{(1)}, q^{(1)})$, that is

$$\boldsymbol{\tau}^{(1)} = -q^{(1)}\mathbf{I} + \nabla\mathbf{v}^{(1)} + (\nabla\mathbf{v}^{(1)})^T, \tag{2.11}$$

$$\mathbf{f} = \mathbf{v}^{(0)}.\nabla\mathbf{v}^{(0)} + \mathbf{v}^{(0)}.\nabla\mathbf{V} + \mathbf{V}.\nabla\mathbf{v}^{(0)}, \tag{2.12}$$

where $\mathbf{I}$ is the idemfactor and the superscript T stands for the transpose of the dyadic; then we can write

$$\nabla.\boldsymbol{\tau}^{(1)} - \mathbf{f} = 0, \tag{2.13}$$

or in summation notation

$$\tau_{jl,j}^{(1)} - f_l = 0. \tag{2.14}$$

Now let us define a new velocity field $(\mathbf{u}, p)$ according to the equations

$$\left.\begin{aligned} &\nabla^2\mathbf{u} - \nabla p = 0, \quad \nabla.\mathbf{u} = 0, \\ &\mathbf{u} = \mathbf{e}_z \quad \text{on} \quad r = 1, \\ &\mathbf{u} = 0 \quad \text{on} \quad \text{the walls}, \\ &\mathbf{u} \to 0 \quad \text{as} \quad r \to \infty, \end{aligned}\right\} \tag{2.15}$$

which is the velocity field for a sphere translating with unit velocity perpendicular to the walls in a quiescent fluid. Denoting the corresponding stress tensor as $\mathbf{t}$, we can write

$$\nabla.\mathbf{t} = 0, \quad \text{or} \quad t_{ij,i} = 0. \tag{2.16}$$

Equations (2.14) and (2.16) then lead trivially to the equations

$$(\tau_{jl,j}^{(1)} - f_l)\,u_l = 0, \quad t_{ij,i}v_j^{(1)} = 0. \tag{2.17a, b}$$

On subtracting (2.17b) from (2.17a) and integrating over the entire fluid volume,

$$\int_{V_f} (\tau^{(1)}_{jl,j} u_l - t_{ij,i} v^{(1)}_j)\, dV = \int_{V_f} f_l u_l\, dV,$$

and rearranging, we obtain

$$\int_{V_f} \left\{ \frac{\partial}{\partial x_j}(\tau^{(1)}_{jl} u_l) - \tau^{(1)}_{jl} \frac{\partial u_l}{\partial x_j} - \frac{\partial}{\partial x_i}(t_{ij} v^{(1)}_j) + t_{ij} \frac{\partial v^{(1)}_j}{\partial x_i} \right\} dV = \int_{V_f} f_l u_l\, dV.$$

Use of the divergence theorem on the first and third terms yields

$$-\int_A n_i(\tau^{(1)}_{ij} u_j - t_{ij} v^{(1)}_j)\, dA - \int_{V_f} \left(\tau^{(1)}_{jl} \frac{\partial u_l}{\partial x_j} - t_{jl} \frac{\partial v^{(1)}_l}{\partial x_j} \right) dV = \int_{V_f} f_l u_l\, dV. \quad (2.18)$$

Here $\mathbf{n}$ denotes the unit vector pointing from the walls and particle surface into the surrounding fluid. By use of the definitions of $\tau^{(1)}_{jl}$ and t_{jl} and the equation of continuity, the integrand in the second integral can be shown to be identically zero. Hence, applying the boundary conditions

$$\mathbf{v}^{(1)} = \mathbf{u} = 0 \quad \text{on} \quad \text{the walls},$$

$$\mathbf{v}^{(1)} \to 0, \quad \mathbf{u} \to 0 \quad \text{as} \quad r \to \infty$$

and

$$v^{(1)}_j = (U^{(1)}_s)_j + \epsilon_{jmk} r_k (\Omega^{(1)}_s)_m, \quad u_j = \delta_{zj} \quad \text{on} \quad r = 1$$

we obtain

$$\int_A n_i \tau^{(1)}_{iz}\, dA - (U^{(1)}_s)_j \int_A n_i t_{ij}\, dA - \epsilon_{jmk} (\Omega^{(1)}_s)_m \int_A r_k n_i t_{ij}\, dA = -\int_{V_f} f_l u_l\, dV. \quad (2.19)$$

The first term on the left-hand side is the z component of the force on the sphere due to the velocity field $(\mathbf{v}^{(1)}, q^{(1)})$. Since the sphere is neutrally buoyant and freely suspended, we require this force to be identically zero, i.e.

$$\int_A n_i \tau^{(1)}_{iz}\, dA = 0.$$

The integral in the second term is nothing more than the hydrodynamic force on the sphere due to $(\mathbf{u}, p)$, i.e. the force on a sphere which translates between and normal to two infinite plane boundaries in a quiescent fluid, while the integral in the third term is the corresponding torque due to $(\mathbf{u}, p)$. The latter is clearly zero in view of the symmetries of the problem (2.15), while we shall show in § 4 that the former is of the form

$$\int_A n_i t_{ij}\, dA = -6\pi[1 + O(\kappa)]\, \delta_{zj}.$$

It thus follows that the migration velocity $U^{(1)}_{sz}$ is given by

$$U^{(1)}_{sz} = -\frac{1}{6\pi} \int_{V_f} f_l u_l\, dV. \quad (2.20)$$

The function $\mathbf{f}$ can be determined completely once the zeroth-order solution $\mathbf{v}^{(0)}$ is available, and the solution of (2.15) is straightforward. Hence, the reciprocal theorem, in the form (2.20), offers a considerably simplified scheme for calculating

the lateral migration velocity, especially when compared with the alternative calculation of the full first-order velocity field $\mathbf{v}^{(1)}$.

It is significant that the same result for the migration velocity $U_{sz}^{(1)}$ can also be obtained to the present level of approximation by a 'two-step' procedure in which one first calculates the force on the sphere with $U_{sz}^{(1)} \equiv 0$. In this case, (2.19) becomes

$$\int_A n_i \tau_{iz}^{(1)} \, dA = -\int_{V_f} f_i u_i \, dV.$$

Thus, the inertia-induced force is given by

$$F_L = -Re \int_{V_f} f_i u_i \, dV. \tag{2.21}$$

Clearly, upon adding the hydrodynamic drag associated with lateral motion

$$-6\pi[1+O(\kappa)]\, Re\, U_{sz}^{(1)}$$

and equating the sum to zero, the expression (2.20) is again obtained. The direct approach represented by the original development leading to (2.20) and the Cox & Brenner (1968) approach involving an intermediate calculation of F_L thus produce identical results to the *present order of approximation*. In view of the historical development of the problem, we shall adopt the latter, two-step calculation.

In the following two sections, we consider solutions of the problems (2.8) and (2.15) for $\mathbf{v}^{(0)}$ and $\mathbf{u}$ which are necessary for evaluation of (2.21).

3. Solution for $(\mathbf{v}^{(0)}, q^{(0)})$

Here we consider the creeping motion of a rigid sphere which is translating with a velocity $U_{sx}^{(0)}\,\mathbf{e}_x$ and rotating with an angular velocity $\Omega_{sy}^{(0)}\,\mathbf{e}_y$ in either simple shear or two-dimensional Poiseuille flow between two parallel plane boundaries. As we have seen, the corresponding velocity field $(\mathbf{v}^{(0)}, q^{(0)})$ is required to evaluate F_L using the reciprocal theorem, equation (2.21).

The solution is found by means of the iterative method of reflexions in which the complete solution $(\mathbf{v}^{(0)}, q^{(0)})$ is constructed as a sum of terms which alternately satisfy boundary conditions on the sphere surface and on the walls. A detailed description is given in Happel & Brenner (1973, chap. 7). The procedure actually produces a sequence of terms of increasing order in κ ($\equiv a/d$) which is convergent for κ small, provided that the sphere is not too close to the walls. Expressing the velocity and pressure fields in the form

$$\left.\begin{aligned} \mathbf{v}^{(0)} &= \mathbf{v}_1^{(0)} + \mathbf{v}_2^{(0)} + \mathbf{v}_3^{(0)} + \ldots, \\ q^{(0)} &= q_1^{(0)} + q_2^{(0)} + q_3^{(0)} + \ldots, \end{aligned}\right\} \tag{3.1}$$

the method of reflexions is defined by the sequence of problems

$$\left.\begin{aligned} &\nabla^2 \mathbf{v}_1^{(0)} - \nabla q_1^{(0)} = 0, \quad \nabla . \mathbf{v}_1^{(0)} = 0, \\ &\mathbf{v}_1^{(0)} = \Omega_{sy}^{(0)}\, \mathbf{e}_y \times \mathbf{r} - (\alpha + \beta z + \gamma z^2 - U_{sx}^{(0)})\, \mathbf{e}_x \quad \text{on} \quad r = 1, \\ &\mathbf{v}_1^{(0)} \to 0 \quad \text{as} \quad r \to \infty; \end{aligned}\right\} \tag{3.2}$$

$$\left.\begin{aligned} &\nabla^2\mathbf{v}_2^{(0)} - \nabla q_2^{(0)} = 0, \quad \nabla\cdot\mathbf{v}_2^{(0)} = 0, \\ &\mathbf{v}_2^{(0)} = -\mathbf{v}_1^{(0)} \quad \text{on} \quad \text{the walls;} \end{aligned}\right\} \tag{3.3}$$

$$\left.\begin{aligned} &\nabla^2\mathbf{v}_3^{(0)} - \nabla q_3^{(0)} = 0, \quad \nabla\cdot\mathbf{v}_3^{(0)} = 0, \\ &\mathbf{v}_3^{(0)} = -\mathbf{v}_2^{(0)} \quad \text{on} \quad r = 1, \\ &\mathbf{v}_3^{(0)} \to 0 \quad \text{as} \quad r \to \infty. \end{aligned}\right\} \tag{3.4}$$

The quantities $\Omega_{sy}^{(0)}$ and $U_{sx}^{(0)}$ are as yet unknowns, which we shall shortly evaluate by equating the net force and torque acting on the sphere owing to $\mathbf{v}^{(0)}$ identically to zero. The field $(\mathbf{v}_1^{(0)}, q_1^{(0)})$ satisfies the boundary condition on the sphere surface, but in doing so generates non-zero terms at the walls. The second term $(\mathbf{v}_2^{(0)}, q_2^{(0)})$ cancels these terms at the wall, but in the process generates a non-zero contribution at the sphere surface which must be cancelled by the third term $(\mathbf{v}_3^{(0)}, q_3^{(0)})$, and so on to higher orders.

The solution for $(\mathbf{v}_1^{(0)}, q_1^{(0)})$ is found by using the general solution of Lamb. The result is

$$\mathbf{v}_1^{(0)} = (u_1^{(0)}, v_1^{(0)}, w_1^{(0)}),$$

$$\begin{aligned} u_1^{(0)} = &-\frac{A_1}{2}\left(1+\frac{x^2}{r^2}\right)\frac{1}{r} - B_1\left(1-\frac{3x^2}{r^2}\right)\frac{1}{r^3} - C_1\frac{z}{r^3} \\ &+\frac{3D_1}{2}\left(\frac{zx^2}{r^5}\right) + 3E_1\left(1-\frac{5x^2}{r^2}\right)\frac{z}{r^5} + 3F_1\left(\frac{z^2-y^2}{r^2}\right)\frac{1}{r^3} \\ &-\frac{G_1}{10}\left(1-\frac{13x^2}{r^2}-\frac{5z^2}{r^2}+\frac{75z^2x^2}{r^4}\right)\frac{1}{r^3} + 3H_1\left(1-\frac{5x^2}{r^2}-\frac{5z^2}{r^2}+\frac{35z^2x^2}{r^4}\right)\frac{1}{r^5}, \end{aligned} \tag{3.5a}$$

$$\begin{aligned} v_1^{(0)} = &-\frac{A_1}{2}\left(\frac{xy}{r^3}\right) + 3B_1\frac{xy}{r^5} + \frac{3D_1}{2}\left(\frac{xyz}{r^5}\right) - 15E_1\frac{xyz}{r^7} + 3F_1\frac{xy}{r^5} \\ &+\frac{G_1}{10}\left(13-\frac{75z^2}{r^2}\right)\frac{xy}{r^5} - 15H_1\left(1-\frac{7z^2}{r^2}\right)\frac{xy}{r^7}, \end{aligned} \tag{3.5b}$$

$$\begin{aligned} w_1^{(0)} = &-\frac{A_1}{2}\left(\frac{zx}{r^3}\right) + 3B_1\frac{zx}{r^5} + C_1\frac{x}{r^3} + \frac{3D_1}{2}\left(\frac{z^2x}{r^5}\right) + 3E_1\left(1-\frac{5z^2}{r^2}\right)\frac{x}{r^5} - 3F_1\frac{zx}{r^5} \\ &+\frac{G_1}{10}\left(23-\frac{75z^2}{r^2}\right)\frac{zx}{r^5} - 15H_1\left(3-\frac{7z^2}{r^2}\right)\frac{zx}{r^7}, \end{aligned} \tag{3.5c}$$

where

$$\left.\begin{aligned} &A_1 = -\tfrac{3}{2}(U_{sx}^{(0)} - \alpha - \tfrac{1}{3}\gamma), \quad B_1 = -\tfrac{1}{4}(U_{sx}^{(0)} - \alpha - \tfrac{3}{5}\gamma), \quad C_1 = -(\Omega_{sy}^{(0)} - \tfrac{1}{2}\beta), \\ &D_1 = -\tfrac{5}{3}\beta, \quad E_1 = -\tfrac{1}{6}\beta, \quad F_1 = -\tfrac{1}{9}\gamma, \quad G_1 = \tfrac{7}{12}\gamma, \quad H_1 = \tfrac{1}{24}\gamma. \end{aligned}\right\} \tag{3.6}$$

The solution for $(\mathbf{v}_2^{(0)}, q_2^{(0)})$ is found by requiring $\mathbf{v}_2^{(0)} = -\mathbf{v}_1^{(0)}$ on the walls. Since the walls are a distance of order κ^{-1} from the sphere, it is convenient to introduce outer variables defined by

$$x' = \kappa x, \quad y' = \kappa y, \quad z' = \kappa z \quad (r' = \kappa r). \tag{3.7}$$

It is then necessary to re-express the field $(\mathbf{v}^{(0)}, q^{(0)})$ in a form appropriate to the region near the walls. This is accomplished by introducing the relationship

$$\frac{1}{r'} = \frac{1}{2\pi}\int_{-\infty}^{\infty}\int_{-\infty}^{\infty} \exp\{i\Omega - |\Lambda|\}\frac{d\xi\, d\eta}{2\zeta}, \tag{3.8}$$

where $\Omega = \frac{1}{2}(\xi x' + \eta y')$, $\Lambda = \frac{1}{2}\zeta z'$ and $\zeta^2 = \xi^2 + \eta^2$, so that the velocity field $\mathbf{v}_1^{(0)}$ can be expressed in integral form as

$$u_1^{(0)} = \frac{1}{2\pi}\int_{-\infty}^{\infty}\int_{-\infty}^{\infty} \exp\{i\Omega - |\Lambda|\}\left[g_1 + \frac{\xi^2}{\zeta^2}(g_2 + |\Lambda|\, g_3)\right] d\xi\, d\eta, \tag{3.9a}$$

$$v_1^{(0)} = \frac{1}{2\pi}\int_{-\infty}^{\infty}\int_{-\infty}^{\infty} \exp\{i\Omega - |\Lambda|\}[g_2 + |\Lambda|\, g_3]\frac{\xi\eta}{\zeta^2}\, d\xi f\eta, \tag{3.9b}$$

$$w_1^{(0)} = \frac{1}{2\pi}\int_{-\infty}^{\infty}\int_{-\infty}^{\infty} \exp\{i\Omega - |\Lambda|\}[g_1 + g_2 + g_3 + |\Lambda|\, g_3]\frac{i\xi}{\zeta}\frac{z'}{|z'|}\, d\xi\, d\eta, \tag{3.9c}$$

where

$$g_1 = -\frac{\kappa}{2\zeta}A_1 - \frac{\kappa^2}{4}\left(C_1 - \frac{D_1}{2}\right)\frac{z'}{|z'|} + \frac{\kappa^3}{4}\left(F_1 - \frac{G_1}{6}\right)\zeta, \tag{3.10a}$$

$$g_2 = \frac{\kappa}{4\zeta}A_1 - \frac{\kappa^3}{8}(B_1 + F_1 + \tfrac{13}{30}G_1)\,\zeta + \frac{\kappa^4}{16}E_1\frac{z'}{|z'|}\zeta^2 - \frac{\kappa^5}{32}H_1\zeta^3, \tag{3.10b}$$

$$g_3 = \frac{\kappa}{4\zeta}A_1 - \frac{\kappa^2 D_1}{8}\frac{z'}{|z'|} + \frac{\kappa^3 G_1}{16}\zeta. \tag{3.10c}$$

In view of the expressions (3.9), the field $\mathbf{v}_2^{(0)}$ may be assumed to have the following form, which satisfies the Stokes and continuity equations:

$$\mathbf{v}_2^{(0)} = (u_2^{(0)}, v_2^{(0)}, w_2^{(0)}),$$

$$u_2^{(0)} = \frac{1}{2\pi}\int_{-\infty}^{\infty}\int_{-\infty}^{\infty} \exp(i\Omega)\left\{\exp(-\Lambda)\left[g_4 + \frac{\xi^2}{\zeta^2}(g_5 + \Lambda g_6)\right] + \exp(\Lambda)\left[g_7 + \frac{\xi^2}{\zeta^2}(g_8 - \Lambda g_9)\right]\right\} d\xi\, d\eta, \tag{3.11a}$$

$$v_2^{(0)} = \frac{1}{2\pi}\int_{-\infty}^{\infty}\int_{-\infty}^{\infty} \exp(i\Omega)\{\exp(-\Lambda)[g_5 + \Lambda g_6] + \exp(\Lambda)[g_8 - \Lambda g_9]\}\frac{\xi\eta}{\zeta^2}\, d\xi\, d\eta, \tag{3.11b}$$

$$w_2^{(0)} = \frac{1}{2\pi}\int_{-\infty}^{\infty}\int_{-\infty}^{\infty} \exp(i\Omega)\{\exp(-\Lambda)[g_4 + g_5 + g_6 + \Lambda g_6] - \exp(\Lambda)[g_7 + g_8 + g_9 - \Lambda g_9]\}\frac{i\xi}{\zeta}\, d\xi\, d\eta. \tag{3.11c}$$

Here, $g_4, g_5, \ldots, g_9$ are unknown functions of ξ and η which are evaluated by applying the boundary conditions $\mathbf{v}_1^{(0)} + \mathbf{v}_2^{(0)} = 0$ on the walls $z' = -s$ and $z' = 1 - s$. In the interest of brevity, the detailed results are not presented here (see Ho 1974); however, results to lowest order in κ will appear in § 5. For our present purposes, it is sufficient to note that $g_4, g_5, \ldots, g_9$ depend on ξ and η only in the combination $\zeta\,[= (\xi^2 + \eta^2)^{\frac{1}{2}}]$ and that they can be expressed in terms of g_1, g_2 and g_3.

In order to solve for $(\mathbf{v}_3^{(0)}, q_3^{(0)})$, it is necessary to evaluate $\mathbf{v}_2^{(0)}$ in the vicinity of the sphere where x' and y' are of order κ. This is achieved by expanding the integrand for small values of $x'^2 + y'^2$. The results are

$$u_2^{(0)} = \tfrac{1}{2}(2I_1 + I_4) - \tfrac{1}{2}\kappa(2I_2 + I_5 - I_7)\,z + \ldots, \tag{3.12a}$$

$$v_2^{(0)} = 0 + \ldots, \tag{3.12b}$$

$$w_2^{(0)} = -\tfrac{1}{2}\kappa(I_2 + I_5 + I_7)\,x + \ldots, \tag{3.12c}$$

where
$$\left.\begin{aligned} I_1 &= \int_0^\infty \zeta(g_4+g_7)\,d\zeta, \quad I_4 = \int_0^\infty \zeta(g_5+g_8)\,d\zeta, \\ I_2 &= \int_0^\infty \tfrac{1}{2}\zeta^2(g_4-g_7)\,d\zeta, \quad I_5 = \int_0^\infty \tfrac{1}{2}\zeta^2(g_5-g_8)\,d\zeta, \\ I_7 &= \int_0^\infty \tfrac{1}{2}\zeta^2(g_6-g_9)\,d\zeta. \end{aligned}\right\} \tag{3.13}$$

With $\mathbf{v}_2^{(0)}$ expressed in this form, $\mathbf{v}_3^{(0)}$ too can be found easily using Lamb's general solution. The result is identical to (3.5) with $A_1, B_1, \ldots, H_1$ replaced by $A_3, B_3, \ldots, H_3$, where

$$\left.\begin{aligned} &A_3 = \tfrac{3}{2}(I_1+\tfrac{1}{2}I_4), \quad B_3 = \tfrac{1}{4}(I_1+\tfrac{1}{2}I_4), \\ &C_3 = -\tfrac{1}{2}\kappa(\tfrac{1}{2}I_2-I_7), \quad D_3 = \tfrac{5}{3}\kappa(\tfrac{3}{2}I_2+I_5), \\ &E_3 = \tfrac{1}{6}\kappa(\tfrac{3}{2}I_2+I_5), \quad F_3, G_3, H_3 = \text{higher order in } \kappa. \end{aligned}\right\} \tag{3.14}$$

This process of satisfying boundary conditions on the sphere and on the walls can be repeated to yield corrections of higher order in κ. For the present purposes, it suffices to stop at $\mathbf{v}_3^{(0)}$.

The hydrodynamic force and torque (dimensionless) acting on the body can be calculated using the formulae (see Happel & Brenner 1973, p. 308)

$$F_x = 4\pi(A_1+A_3+\ldots), \quad T_y = 8\pi(C_1+C_3+\ldots), \tag{3.15a, b}$$

for which the coefficients A_1, A_3, C_1 and C_3 are previously listed in (3.6) and (3.14). It is obvious that, since $(\mathbf{v}^{(0)}, p^{(0)})$ corresponds to Stokes flow, the force and torque on the sphere are in the x direction and y direction, respectively. It is most convenient to re-express the coefficients A_3 and C_3 in terms of A_1, C_1 and D_1, i.e.

$$A_3 \equiv \tfrac{3}{2}(I_1+\tfrac{1}{2}I_4) = \kappa A_1 K_A + \kappa^2 C_1 K_C + \kappa^2 D_1 K_D + \ldots, \tag{3.16a}$$

$$C_3 \equiv -\tfrac{1}{2}\kappa(\tfrac{1}{2}I_2-I_7) = \kappa^2 A_1 L_A + \kappa^3 C_1 L_C + \kappa^3 D_1 L_D + \ldots. \tag{3.16b}$$

Thus, substituting for A_1, C_1 and D_1 from (3.6), the force and torque may be written as

$$F_x/4\pi = -\tfrac{3}{2}(U_{sx}^{(0)} - \alpha - \tfrac{1}{3}\kappa^2\gamma')(1+\kappa K_A) - \kappa^2(\Omega_{sy}^{(0)} - \tfrac{1}{2}\kappa\beta')K_C - \tfrac{5}{3}\kappa^3\beta' K_D + \ldots, \tag{3.17a}$$

$$T_y/8\pi = -(\Omega_{sy}^{(0)} - \tfrac{1}{2}\kappa\beta')(1+\kappa^3 L_C) - \tfrac{3}{2}\kappa^2(U_{sx}^{(0)} - \alpha - \tfrac{1}{3}\kappa^2\gamma')L_A - \tfrac{5}{3}\kappa^4\beta' L_D + \ldots. \tag{3.17b}$$

The coefficients K_A, K_C, K_D, L_A, L_C and L_D are integrals over ζ which are of order κ^0, and are dependent only on the parameter s. In addition, $\beta' = \beta/\kappa = O(1)$ and $\gamma' = \gamma/\kappa^2 = O(1)$. Equations (3.17$a$) and (3.17$b$) may be used to calculate the force and torque acting on a sphere which is translating and rotating at a known *specified* rate in either Couette or two-dimensional Poiseuille flow. Alternatively, the force and torque may be specified and (3.17a) and (3.17b) used to determine the corresponding translational and rotational velocities $U_{sx}^{(0)}$ and $\Omega_{sy}^{(0)}$.

s	Present theory, $-\frac{10}{9}K_D$	Halow & Wills, $\frac{5}{16}[1/(1-s)^2-1/s^2]$	Wakiya
0·10	−30·834	−30·864	—
0·20	−7·199	−7·324	—
0·25	−4·315	−4·444	−4·315
0·30	−2·717	−2·835	—
0·40	−1·018	−1·085	—
0·50	0·0	0·0	—

TABLE 1. The slip velocity $U_p/V_w\kappa^3$ of a neutrally buoyant sphere freely suspended in a simple shear flow bounded between two walls, $K_D(s) = -K_D(1-s)$.

The specific case of primary interest in the present context is $F_x = T_y = 0$, corresponding to a freely suspended neutrally buoyant particle. In this case, it can be shown from (3.17*a*) and (3.17*b*) that

$$U_{sx}^{(0)} - \alpha = \tfrac{1}{3}\kappa^2\gamma' - \tfrac{10}{9}\kappa^3\beta' K_D, \tag{3.18a}$$

$$\Omega_{sy}^{(0)} - \tfrac{1}{2}\kappa\beta' = -\tfrac{5}{3}\kappa^4\beta' L_D. \tag{3.18b}$$

Thus, the sphere rotates with the vorticity of the fluid to within a small correction $O(\kappa^4)$. In two-dimensional Poiseuille flow

$$\alpha = 4V_{\max}s(1-s), \quad \beta' = 4V_{\max}(1-2s), \quad \gamma' = -4V_{\max}.$$

Hence, the slip velocity $U_p \equiv U_{sx}^{(0)} - \alpha$ becomes

$$U_p = -\tfrac{4}{3}V_{\max}\kappa^2 - \tfrac{40}{9}V_{\max}\kappa^3(1-2s)K_D + O(\kappa^4). \tag{3.19}$$

This expression is consistent with the similar result given in Happel & Brenner (1973, chap. 3) for motion through a circular tube, and predicts that a small sphere (i.e. $\kappa \ll 1$) will lag behind the surrounding fluid for all positions s. In simple shear flow

$$\alpha = V_w s, \quad \beta' = V_w, \quad \gamma' = 0,$$

so that

$$U_p = -\tfrac{10}{9}V_w\kappa^3 K_D + O(\kappa^4). \tag{3.20}$$

We have numerically evaluated K_D for various values of s and the results are listed in table 1. It is evident that the sphere *leads* the fluid for $s > 0{\cdot}5$ and *lags* behind it for $s < 0{\cdot}5$. We note also the expected symmetry in K_D:

$$K_D(s) = -K_D(1-s).$$

These results for simple shear flow may be compared with the similar calculation of Wakiya (1956), who solved the same problem but evaluated U_p only for $s = 0{\cdot}25$ and $0{\cdot}75$. As indicated in table 1, our calculated values are essentially identical to his at those values of s. More recently, Halow & Wills (1970*a*) used an *ad hoc* method in which the contributions of the two individual walls were summed to estimate the force acting on a sphere between two plane walls. The resulting formula for F_x is

$$\frac{F_x}{6\pi} = -(U_{sx}^{(0)} - \alpha)\left\{1 + \tfrac{9}{16}\kappa\left[\frac{1}{s} + \frac{1}{1-s}\right]\right\} - \tfrac{5}{16}V_w k^3\left[\frac{1}{s^2} - \frac{1}{(1-s)^2}\right]. \tag{3.21}$$

	(a)			(b)		
s	Present theory, K_A	Halow & Wills, $\frac{9}{16}[1/s+1/(1-s)]$	Faxen	Present theory, L_A	Faxen	Wakiya
0·10	5·709	6·250	—	0·236	—	—
0·20	3·073	3·516	—	0·286	—	—
0·25	2·611	3·000	2·610	0·270	0·267	0·270
0·30	2·338	2·679	—	0·235	—	—
0·40	2·076	2·344	—	0·129	—	—
0·50	2·008	2·250	—	0·0	—	—

TABLE 2. (*a*) Additional hydrodynamic resistance on a sphere translating parallel to two infinite plane walls, $K_A(s) = K_A(1-s)$; and (*b*) the induced angular velocity,

$$L_A(s) = -L_A(1-s).$$

The corresponding values for $U_p/V_w\kappa^3$ are also listed in table 1 for the case in which $F_x = T_y = 0$. Sufficiently near the walls, $s < 0{\cdot}15$ or $s > 0{\cdot}85$, *both* theories reduce, in effect, to the motion of a sphere near a single plane wall and agreement between them is expected. Surprisingly, however, the simple addition of the two single-wall corrections gives results which compare quite well with our present 'exact' results for *all* values of s.

Although not required in the present context, it is also of general interest to use (3.17*a*) and (3.17*b*) to calculate the force and torque on a sphere which is translating in the x direction and/or rotating in the y direction between two infinite plane walls in a quiescent fluid. In these circumstances, since

$$\alpha = \beta' = \gamma' = 0,$$

$$F_x = -6\pi U_{sx}^{(0)}(1+\kappa K_A) - 4\pi\kappa^2\Omega_{sy}^{(0)} K_C, \tag{3.22a}$$

$$T_y = -8\pi\Omega_{sy}^{(0)}(1+\kappa^3 L_C) - 12\pi\kappa^2 U_{sx}^{(0)} L_A. \tag{3.22b}$$

In particular, a freely rotating sphere which is rising (or settling) through a quiescent fluid will experience the usual Stokes drag force modified by the additional term κK_A, and in addition will undergo an induced rotation at a rate

$$\Omega_{sy}^{(0)} = -\tfrac{3}{2}\kappa^2 U_{sx}^{(0)} L_A. \tag{3.23}$$

The coefficients K_A and L_A are listed in table 2 for various values of s. The values of the term corresponding to K_A, i.e. $\frac{9}{16}[1/s+1/(1-s)]$, from the approximate method, equation (3.21), are also listed in the same table. Wakiya (1956) and Faxen (see Happel & Brenner 1973, chap. 7) also reported the coefficients K_A and L_A for $s = 0{\cdot}25$ and $0{\cdot}75$ (see table 2).

4. Solution for $(\mathbf{u}, p)$

We now consider the creeping motion of a rigid sphere which is translating in a quiescent fluid between two parallel plane boundaries in the direction perpendicular to them. This velocity field $(\mathbf{u}, p)$ is required in the integral

expression (2.21) for the lateral force. The method of solution is identical to that of the preceding section, hence only the results will be given. We express $(\mathbf{u}, p)$ as

$$\left.\begin{aligned}\mathbf{u} &= \mathbf{u}_1+\mathbf{u}_2+\mathbf{u}_3+\ldots,\\ p &= p_1+p_2+p_3+\ldots.\end{aligned}\right\} \tag{4.1}$$

The solution $\mathbf{u}_1$ satisfying the boundary condition on the sphere, i.e. $\mathbf{u}_1 = \mathbf{e}_z$ at $r = 1$, is

$$\mathbf{u}_1 = (u_1, v_1, w_1),$$

$$u_1 = -\frac{A_1}{2}\frac{zx}{r^3}+3B_1\frac{zx}{r^5}, \quad v_1 = -\frac{A_1}{2}\frac{yz}{r^3}+3B_1\frac{yz}{r^5}, \tag{4.2a, b}$$

$$w_1 = -\frac{A_1}{2}\left(1+\frac{z^2}{r^2}\right)\frac{1}{r}-B_1\left(1-\frac{3z^2}{r^2}\right)\frac{1}{r^3}, \tag{4.2c}$$

and

$$A_1 = -\tfrac{3}{2}, \quad B_1 = -\tfrac{1}{4}. \tag{4.3}$$

Using (3.8), an integral form for $\mathbf{u}_1$ can be obtained in terms of the outer variables x', y', z' and r':

$$u_1 = \frac{1}{2\pi}\int_{-\infty}^{\infty}\int_{-\infty}^{\infty}\exp\{i\Omega-|\Lambda|\}\left[|z'|f_1+\frac{2}{\zeta}f_2\right]\frac{i\xi}{2}\frac{z'}{|z'|}\,d\xi\,d\eta, \tag{4.4a}$$

$$v_1 = \frac{1}{2\pi}\int_{-\infty}^{\infty}\int_{-\infty}^{\infty}\exp\{i\Omega-|\Lambda|\}\left[|z'|f_1+\frac{2}{\zeta}f_2\right]\frac{i\eta}{2}\frac{z'}{|z'|}\,d\xi\,d\eta, \tag{4.4b}$$

$$w_1 = \frac{-1}{2\pi}\int_{-\infty}^{\infty}\int_{-\infty}^{\infty}\exp\{i\Omega-|\Lambda|\}[f_1+f_2+|\Lambda|f_1]\,d\xi\,d\eta, \tag{4.4c}$$

where

$$f_1 = \kappa A_1/4\zeta, \quad f_2 = -\tfrac{1}{8}\kappa^3 B_1\zeta. \tag{4.5a, b}$$

Again, $\mathbf{u}_2$ is assumed to have the form $\mathbf{u}_2 = (u_2, v_2, w_2)$, with

$$u_2 = \frac{1}{2\pi}\int_{-\infty}^{\infty}\int_{-\infty}^{\infty}\exp(i\Omega)\left\{\exp(-\Lambda)\left[z'f_3+\frac{2}{\zeta}f_4\right]+\exp(\Lambda)\left[z'f_5-\frac{2}{\zeta}f_6\right]\right\}\frac{i\xi}{2}\,d\xi\,d\eta, \tag{4.6a}$$

$$v_2 = \frac{1}{2\pi}\int_{-\infty}^{\infty}\int_{-\infty}^{\infty}\exp(i\Omega)\left\{\exp(-\Lambda)\left[z'f_3+\frac{2}{\zeta}f_4\right]+\exp(\Lambda)\left[z'f_5-\frac{2}{\zeta}f_6\right]\right\}\frac{i\eta}{2}\,d\xi\,d\eta, \tag{4.6b}$$

$$w_2 = \frac{-1}{2\pi}\int_{-\infty}^{\infty}\int_{-\infty}^{\infty}\exp(i\Omega)\{\exp(-\Lambda)[f_3+f_4+\Lambda f_3] + \exp(\Lambda)[f_5+f_6-\Lambda f_5]\}\,d\xi\,d\eta. \tag{4.6c}$$

The coefficients f_3, f_4, f_5 and f_6 are found by satisfying the boundary condition $\mathbf{u}_1+\mathbf{u}_2 = 0$ on the walls $z' = -s$ and $z' = 1-s$. As before, the detailed results are omitted (see Ho 1974) while the expressions to the lowest order in κ are given in § 5. Again, f_3, f_4, f_5 and f_6 are found to be dependent on ζ. Near the sphere $\mathbf{u}_2$ can be simplified to the form

$$u_2 = -\tfrac{1}{2}\kappa J_2 x+O(\kappa^3), \quad v_2 = -\tfrac{1}{2}\kappa J_2 y+O(\kappa^3), \tag{4.7a, b}$$

$$w_2 = -(J_1+J_4)+\kappa J_2 z+O(\kappa^3), \tag{4.7c}$$

where

$$\left.\begin{aligned}J_1 = \int_0^{\infty}\zeta(f_4+f_6)\,d\zeta, \quad J_4 = \int_0^{\infty}\zeta(f_3+f_5)\,d\zeta,\\ J_2 = \int_0^{\infty}\tfrac{1}{2}\zeta^2(f_4-f_6)\,d\zeta.\end{aligned}\right\} \tag{4.8}$$

s	K_A	$\frac{9}{8}[1/s+1/(1-s)]$
0·1	11·2	12·50
0·2	5·65	7·03
0·25	4·560	6·000
0·3	3·864	5·357
0·4	3·117	4·688
0·5	2·902	4·500

TABLE 3. Additional hydrodynamic resistance on a sphere translating perpendicular to two infinite plane walls, $K_A(s) = K_A(1-s)$.

Hence, the solution $\mathbf{u}_3$ satisfying the boundary condition $\mathbf{u}_2+\mathbf{u}_3 = 0$ on $r = 1$ is the same as (4.2) with A_1 and B_1 replaced by A_3 and B_3, where

$$A_3 = -\tfrac{3}{2}(J_1+J_4), \quad B_3 = -\tfrac{1}{4}(J_1+J_4). \tag{4.9}$$

This completes the solution to the order of approximation required for our purposes.

As in the previous case, the force acting on the particle can be calculated from the coefficients A_1 and A_3 for any given imposed velocity. The torque is identically zero. The general form for the force is

$$F_z = 4\pi(A_1+A_3+\ldots). \tag{4.10}$$

Hence, substituting for A_1 and A_3 from (4.3) and (4.9), and noting that

$$A_3 \equiv -\tfrac{3}{2}(J_1+J_4) = \kappa A_1 K_A + \kappa^3 B_1 K_B, \tag{4.11}$$

we obtain

$$F_z/6\pi = -(1+\kappa K_A), \tag{4.12}$$

where the coefficient K_A is an integral over ζ which is $O(1)$ in κ, and is a function of the single parameter s. Thus, to a first approximation we obtain the usual Stokes force, with a correction $O(\kappa)$ due to the presence of the walls. The coefficient K_A is listed as a function of s in table 3. So far as we are aware, the only directly comparable results for two walls are from the study of Halow & Wills (1970*a*), who approximated the drag force as the sum of two single-wall calculations. This approach yields

$$\frac{F_z}{6\pi} = -\left[1+\tfrac{9}{8}\kappa\left(\frac{1}{s}+\frac{1}{1-s}\right)\right], \tag{4.13}$$

which is to be compared with (4.12). We have listed the correction term from (4.13) in a form comparable with the coefficient K_A in table 3. Unlike the previous example, where the *ad hoc* method of Halow & Wills produces reasonably accurate results, the comparison in this case is very poor with the values of the exact calculation being as much as 50 % lower than the values from (4.13). As one would expect, the greatest differences occur near the centre of the gap, where the influences of the walls are comparable. When the particle is close to one wall, the influence of the other is apparently weak and the one-wall approximation is adequate.

5. The lateral force

To calculate the lateral force, the volume integral (2.21) must be evaluated using the velocity fields $\mathbf{v}^{(0)}$ and $\mathbf{u}$ of the preceding two sections, i.e. we require

$$F_L = -Re\int_{V_f} \mathbf{u}.[\mathbf{v}^{(0)}.\nabla\mathbf{v}^{(0)} + \mathbf{v}^{(0)}.\nabla\mathbf{V} + \mathbf{V}.\nabla\mathbf{v}^{(0)}]\,dV,$$

where V_f is the fluid volume outside the sphere and bounded between the walls:

$$V_f = \{\mathbf{r} | r \geqslant 1,\ x < \infty,\ y < \infty,\ -s/\kappa \leqslant z \leqslant (1-s)/\kappa\}.$$

Motivated by the fact that the lower limit of integration is $O(1)$ while the upper limit is $O(1/\kappa)$, we divide the region of integration into two domains V_1 and V_2 such that

$$V_1 = \{\mathbf{r} | 1 \leqslant r < \lambda\kappa^{\chi-1}\}, \tag{5.1}$$

$$V_2 = \{\mathbf{r} | \lambda\kappa^{\chi-1} \leqslant r < \infty,\ -s/\kappa \leqslant z \leqslant (1-s)/\kappa\}, \tag{5.2}$$

where $0 < \chi < 1$ and λ is a constant of order κ^0. Hence

$$F_L = -Re\int_{V_1} \mathbf{u}.\mathbf{f}\,dV - Re\int_{V_2} \mathbf{u}.\mathbf{f}\,dV. \tag{5.3}$$

Let us now investigate the magnitude of the first integral in (5.3). The solutions of the previous two sections and the general form (2.2) of the undisturbed flow field give the following orders of magnitude in κ and the radial position r:

$$\left.\begin{aligned} \mathbf{u} &= \mathbf{u}_1 + \mathbf{u}_2 + \mathbf{u}_3 + \ldots, \\ \mathbf{u}_1 &\sim O(1/r) + O(1/r^3), \\ \mathbf{u}_2 &\sim O(\kappa) + O(\kappa^2 r) + \ldots, \\ \mathbf{u}_3 &\sim O\left(\frac{\kappa}{r}\right) + O\left(\frac{\kappa}{r^3}\right) + O\left(\frac{\kappa^2}{r^2}\right) + O\left(\frac{\kappa^2}{r^4}\right) + \ldots, \end{aligned}\right\} \tag{5.4a}$$

$$\left.\begin{aligned} \mathbf{v}^{(0)} &= \mathbf{v}_1^{(0)} + \mathbf{v}_2^{(0)} + \mathbf{v}_3^{(0)} + \ldots, \\ \mathbf{v}_1^{(0)} &\sim O\left(\frac{\kappa}{r^2}\right) + O\left(\frac{\kappa}{r^4}\right) + O\left(\frac{\kappa^2}{r^3}\right) + O\left(\frac{\kappa^2}{r^5}\right) + O\left(\frac{\kappa^3}{r}\right) + O\left(\frac{\kappa^3}{r^3}\right) + \ldots, \\ \mathbf{v}_2^{(0)} &\sim O(\kappa^3) + O(\kappa^4 r) + \ldots, \\ \mathbf{v}_3^{(0)} &\sim O\left(\frac{\kappa^3}{r}\right) + O\left(\frac{\kappa^3}{r^3}\right) + O\left(\frac{\kappa^4}{r^2}\right) + O\left(\frac{\kappa^4}{r^4}\right) + \ldots, \end{aligned}\right\} \tag{5.4b}$$

$$\mathbf{V} \sim O(\kappa r) + O(\kappa^2 r^2). \tag{5.4c}$$

It follows, therefore, that the integrand behaves as

$$\mathbf{u}.\mathbf{f} \sim \kappa^2 O\left(\frac{1}{r^3}, \frac{1}{r^5}, \frac{1}{r^7}\right) + \kappa^3 O\left(\frac{1}{r^2}, \frac{1}{r^3}, \frac{1}{r^4}, \ldots\right) + \ldots. \tag{5.5}$$

It can be shown that the volume integral over a spherical shell (i.e. $1 \leqslant r < \lambda\kappa^{\chi-1}$) of the first term in (5.5) is identically zero. Thus, the dominant term derives from the term of order κ^3/r^2 in the integrand and the magnitude of the integral over V_1 is

$$\int_{V_1} \mathbf{u}.\mathbf{f}\,dV = O(\kappa^{\chi+2}). \tag{5.6}$$

Now let us investigate the second integral in (5.3). Here, in estimating the magnitudes of the various velocity fields, it is convenient to use the outer variables x', y', z' and r'. It is then easily shown that

$$\mathbf{u}_1 \sim O(\kappa), \quad \mathbf{u}_2 \sim O(\kappa), \quad \mathbf{u}_3 \sim O(\kappa^2), \tag{5.7}$$

$$\mathbf{v}_1^{(0)} \sim O(\kappa^3), \quad \mathbf{v}_2^{(0)} \sim O(\kappa^3), \quad \mathbf{v}_3^{(0)} \sim O(\kappa^4), \tag{5.8}$$

$$\mathbf{V} \sim O(1). \tag{5.9}$$

Hence, neglecting terms $O(\kappa^3)$ and smaller, the second volume integral of (5.3) can be written as

$$-Re\int_{V_2} \mathbf{u}.\mathbf{f}\,dV = -Re\,\kappa^{-2}\int_{V_2} (\mathbf{u}_1+\mathbf{u}_2).[(\mathbf{v}_1^{(0)}+\mathbf{v}_2^{(0)}).\nabla\mathbf{V} + \mathbf{V}.\nabla(\mathbf{v}_1^{(0)}+\mathbf{v}_2^{(0)})]\,dV + O(\kappa^3), \tag{5.10}$$

where the velocities are expressed in *outer variables* and V_2 is the volume element defined by

$$\lambda\kappa^{\chi} \leqslant r'$$

and

$$x' < \infty, \quad y' < \infty, \quad -s \leqslant z' \leqslant (1-s). \tag{5.11}$$

Now, the dominant term in the integrand of (5.10), as $r' \to 0$, is $O(\kappa^4/r'^2)$, hence if the lower limit $r' = \lambda\kappa^{\chi}$ were replaced by $r' = 0$, an error would be introduced which would be of the same order of magnitude as the contribution from V_1, i.e. $\kappa^{-2}\int O(\kappa^4/r'^2)\,dr'^3 = O(\kappa^{2+\chi})$. But the volume integral over V_2 is of order κ^2, hence to a first approximation, it is permissible to put $r' = 0$ as the lower limit and neglect the integral over V_1 entirely. We note that the resultant expression for F_L, equation (5.10), involves only $\mathbf{u}_1$ and $\mathbf{u}_2$ of $\mathbf{u}$, $\mathbf{v}_1^{(0)}$ and $\mathbf{v}_2^{(0)}$ of $\mathbf{v}^{(0)}$, and a single term of $\mathbf{V}$. Let us rewrite these various velocity fields (in terms of outer variables x', y', z' and r'). First, $\mathbf{u}$ is given by $\mathbf{u} = \mathbf{u}_1 + \mathbf{u}_2$, with

$$\mathbf{u}_1 = (u_1, v_1, w_1),$$

$$u_1 = \kappa\, 3z'x'/4r'^3 + O(\kappa^3), \quad v_1 = \kappa\, 3y'z'/4r'^3 + O(\kappa^3), \tag{5.12a, b}$$

$$w_1 = \kappa\frac{3}{4}\left(1+\frac{z'^2}{r'^2}\right)\frac{1}{r'} + O(\kappa^3), \tag{5.12c}$$

$$\mathbf{u}_2 = (u_2, v_2, w_2),$$

$$u_2 = -\frac{x'}{\rho'}\int_0^{\infty} J_1(W)\,[\exp(-\Lambda)\,(\Lambda f_3 + f_4) + \exp(\Lambda)\,(\Lambda f_5 - f_6)]\,\zeta\,d\zeta, \tag{5.13a}$$

$$v_2 = -\frac{y'}{\rho'}\int_0^{\infty} J_1(W)\,[\exp(-\Lambda)\,(\Lambda f_3 + f_4) + \exp(\Lambda)\,(\Lambda f_5 - f_6)]\,\zeta\,d\zeta, \tag{5.13b}$$

$$w_2 = -\int_0^{\infty} J_0(W)\,[\exp(-\Lambda)\,(f_3 + f_4 + \Lambda f_3) + \exp(\Lambda)\,(f_5 + f_6 - \Lambda f_5)]\,\zeta\,d\zeta, \tag{5.13c}$$

where

$$f_3 = (3\kappa/8\Delta\zeta)\,[(t_2-1)\,(t-1) + (1-s)\,\zeta t_2 - \zeta t + s\zeta t_2 t - (1-s)\,\zeta^2 t] + O(\kappa^3), \tag{5.14a}$$

$$f_4 = (-3\kappa/16\Delta\zeta)\,[(1-s)^2\,\zeta^2 t_2 - (1-2s)\,\zeta^2 t - s^2\zeta^2 t_2 t + s(1-s)\,\zeta^3 t] + O(\kappa^3), \tag{5.14b}$$

$$f_5 = (3\kappa/8\Delta\zeta)\,[(t_1-1)\,(t-1) + s\zeta t_1 - \zeta t + (1-s)\,\zeta t_1 t - s\zeta^2 t] + O(\kappa^3), \tag{5.14c}$$

$$f_6 = (-3\kappa/16\Delta\zeta)\,[s^2\zeta^2 t_1 + (1-2s)\,\zeta^2 t - (1-s)^2\,\zeta^2 t_1 t + s(1-s)\,\zeta^3 t] + O(\kappa^3) \tag{5.14d}$$

and

$$\rho'^2 = x'^2+y'^2, \quad t = \exp\zeta, \quad t_1 = \exp s\zeta, \quad t_2 = \exp[(1-s)\zeta], \quad \Delta = (t-1)^2-\zeta^2 t,$$

$W = \frac{1}{2}\zeta\rho'$ and the $J_n(W)$ are Bessel functions of the first kind of order n.

Second, $\mathbf{v}^{(0)}$ is given by $\mathbf{v}^{(0)} = \mathbf{v}_1^{(0)} + \mathbf{v}_2^{(0)}$, with

$$\mathbf{v}_1^{(0)} = (u_1^{(0)}, v_1^{(0)}, w_1^{(0)}),$$

$$u_1^{(0)} = \frac{3\kappa^2 D_1}{2}\left(\frac{z'x'^2}{r'^5}\right) - \frac{\kappa A_1}{2}\left(1+\frac{x'^2}{r'^2}\right)\frac{1}{r'} - \frac{\kappa^2 C_1 z'}{r'^3}, \tag{5.15a}$$

$$v_1^{(0)} = \frac{3\kappa^2 D_1}{2}\left(\frac{x'y'z'}{r'^5}\right) - \frac{\kappa A_1}{2}\left(\frac{x'y'}{r'^3}\right), \tag{5.15b}$$

$$w_1^{(0)} = \frac{3\kappa^2 D_1}{2}\left(\frac{z'^2x'}{r'^5}\right) - \frac{\kappa A_1}{2}\left(\frac{z'x'}{r'^3}\right) + \frac{\kappa^2 C_1 x'}{r'^3}, \tag{5.15c}$$

with $D_1 = -\frac{5}{3}\beta'\kappa$, $A_1 = -\frac{3}{2}(U_{sx}^{(0)} - \alpha - \frac{1}{3}\gamma'\kappa^2)$ and $C_1 = -(\Omega_{sy}^{(0)} - \frac{1}{2}\beta'\kappa)$. Hence, from (3.18), it follows, for a freely suspended neutrally buoyant sphere, that

$$A_1 = \tfrac{5}{3}\beta'\kappa^3 K_D \quad \text{and} \quad C_1 = \tfrac{5}{3}\beta'\kappa^4 L_D,$$

so that, in (5.15), the term involving D_1 is $O(\kappa^3)$, the term involving A_1 is $O(\kappa^4)$ and the term involving C_1 is $O(\kappa^6)$:

$$u_1^{(0)} = -\frac{5\kappa^3\beta'}{2}\left(\frac{z'x'^2}{r'^5}\right) - \frac{5\kappa^4\beta' K_D}{6}\left(1+\frac{x'^2}{r'^2}\right)\frac{1}{r'} - \frac{5\kappa^6\beta' L_D z'}{3r'^3}, \tag{5.16a}$$

$$v_1^{(0)} = -\frac{5\kappa^3\beta'}{2}\left(\frac{x'y'z'}{r'^5}\right) - \frac{5\kappa^4\beta' K_D}{6}\left(\frac{x'y'}{r'^3}\right), \tag{5.16b}$$

$$w_1^{(0)} = -\frac{5\kappa^3\beta'}{2}\left(\frac{z'^2x'}{r'^5}\right) - \frac{5\kappa^4\beta' K_D}{6}\left(\frac{z'x'}{r'^3}\right) + \frac{5\kappa^6\beta' L_D x'}{3r'^3}. \tag{5.16c}$$

The velocity field $\mathbf{v}_2^{(0)}$ is given by

$$\mathbf{v}_2^{(0)} = (u_2^{(0)}, v_2^{(0)}, w_2^{(0)}),$$

$$u_2^{(0)} = \int_0^\infty \left\{\tfrac{1}{2}J_0(W)[\exp(-\Lambda)(2g_4+g_5+\Lambda g_6)+\exp(\Lambda)(2g_7+g_8-\Lambda g_9)]\right.$$
$$\left. -\frac{1}{2}\frac{x'^2-y'^2}{\rho'^2}J_2(W)[\exp(-\Lambda)(g_5+\Lambda g_6)+\exp(\Lambda)(g_8-\Lambda g_9)]\right\}\zeta\,d\zeta, \tag{5.17a}$$

$$v_2^{(0)} = -\int_0^\infty \frac{x'y'}{\rho'^2}J_2(W)[\exp(-\Lambda)(g_5+\Lambda g_6)+\exp(\Lambda)(g_8-\Lambda g_9)]\zeta\,d\zeta, \tag{5.17b}$$

$$w_2^{(0)} = -\int_0^\infty \frac{x'}{\rho'}J_1(W)[\exp(-\Lambda)(g_4+g_5+g_6+\Lambda g_6)-\exp(\Lambda)(g_7+g_8+g_9-\Lambda g_9)]\zeta\,d\zeta. \tag{5.17c}$$

Here, $g_4(\zeta), g_5(\zeta), \ldots, g_9(\zeta)$ are expressible in terms of g_1, g_2 and g_3, which are given by

$$g_1 = -\frac{\kappa A_1}{2\zeta} + \frac{\kappa^2 D_1 z'}{8|z'|} - \frac{\kappa^2 C_1 z'}{4|z'|} + \ldots, \tag{5.18a}$$

$$g_2 = \frac{\kappa A_1}{4\zeta} + \ldots, \quad g_3 = \frac{\kappa A_1}{4\zeta} - \frac{\kappa^2 D_1 z'}{8|z'|} + \ldots. \tag{5.18b, c}$$

For a neutrally buoyant particle, the term involving D_1 is $O(\kappa^3)$, the term involving A_1 is $O(\kappa^4)$ and the term involving C_1 is $O(\kappa^6)$; then it can be shown that to the lowest order in κ

$$g_4 = -\frac{5\kappa^3\beta'}{24}\left(\frac{t_2+1}{t-1}\right)+O(\kappa^4), \tag{5.19a}$$

$$g_5 = \frac{5\kappa^3\beta'}{48}\left\{\frac{t_2+1+(1-s)\zeta}{t-1}-\frac{1}{\Delta}\right.$$
$$\times[(t_2+1)(t-1)-2(1-s)\zeta t_2-(1+s)\zeta t-2s\zeta t_2 t-(1-s)\zeta]$$
$$\left.-\frac{\zeta^2}{\Delta(t-1)}[(1-s)^2 t_2+2s(1-s)t_2 t+t^2+s^2 t_2 t^2-(1-s)^2\zeta t-s(1-s)\zeta t^2]\right\}+O(\kappa^4), \tag{5.19b}$$

$$g_6 = (5\kappa^3\beta'/24\Delta)[(t_2+1)(t-1)-(1-s)\zeta t_2-\zeta t-s\zeta t_2 t+(1-s)\zeta^2 t]+O(\kappa^4), \tag{5.19c}$$

$$g_7 = \frac{5\kappa^3\beta'}{24}\left(\frac{t_1+1}{t-1}\right)+O(\kappa^4), \tag{5.19d}$$

$$g_8 = -\frac{5\kappa^3\beta'}{48}\left\{\frac{t_1+1+s\zeta}{t-1}-\frac{1}{\Delta}[(t_1+1)(t-1)-2s\zeta t_1-(2-s)\zeta t-2(1-s)\zeta t_1 t-s\zeta]\right.$$
$$\left.-\frac{\zeta^2}{\Delta(t-1)}[s^2 t_1+2s(1-s)t_1 t+t^2+(1-s)^2 t_1 t^2-s^2\zeta t-s(1-s)\zeta t^2]\right\}+O(\kappa^4), \tag{5.19e}$$

$$g_9 = (-5\kappa^3\beta'/24\Delta)[(t_1+1)(t-1)-s\zeta t_1-\zeta t-(1-s)\zeta t_1 t+s\zeta^2 t]+O(\kappa^4). \tag{5.19f}$$

Finally, the undisturbed velocity field **V** is

$$\mathbf{V} = (\beta' z'+\gamma' z'^2)\,\mathbf{e}_x+O(\kappa^2). \tag{5.20}$$

It may now be seen from (5.15) and (5.16) that the dominant term in the expression (5.10) for *neutrally buoyant particles* is due to the stresslet (D_1, determined by the bulk rate of strain) and its reflexion off the walls. The *Stokeslet* contribution (A_1, originating from the lag velocity) and the *couplet* contribution (C_1, originating from the rotation slip) are of one and three orders of magnitude smaller in κ, and hence may be neglected for this case. From this, one can conclude that the lateral force originates from the shear field acting on the sphere rather than the presence of a wall-induced lag velocity or slip–spin. On the other hand, it should be pointed out that for the special case of a non-rotating sphere, where $C_1 = \frac{1}{2}\kappa\beta'$, the stresslet and couplet terms are of same order of magnitude. Similarly, if the lag velocity were significantly larger, as might be the case for a non-neutrally buoyant sphere, the contribution of the Stokeslet term might generate a lateral force of comparable or even larger magnitude than that determined here. Indeed, it is clear from (5.15) and (5.16) that a suitable criterion for neglect of the contribution to the lateral force induced by the body force (for a vertical flow channel) is

$$|\kappa^2 D_1| \gg |\kappa A_1| \quad \text{or} \quad |A_1| \ll \kappa^2\beta'. \tag{5.21}$$

An explicit requirement for the case where $T_y = 0$ follows immediately from (3.17a) and (3.17b), which yield

$$A_1 = (F_x/4\pi + \tfrac{5}{3}\kappa^3\beta' K_D)(1+O(\kappa)).$$

That is, we require $$|F_x/4\pi| \ll \kappa^2\beta'. \tag{5.22}$$

When the body force is gravity, (5.22) becomes (in dimensional quantities)

$$a^2|\rho_s - \rho_0|\, g \ll \mu_0 V_m^* \kappa^2, \tag{5.23}$$

in which g is the gravitational acceleration, ρ_s is the density of the particle, ρ_0 is the density of the suspending fluid and V_m^* is the dimensional mean flow rate, being equal to $\frac{1}{2}V_w^*$ for simple shear flow and $\frac{2}{3}V_{\max}^*$ for two-dimensional Poiseuille flow.

We have used the various estimates (5.12)–(5.20) to evaluate the expression (5.10), leading to the lateral force F_L. As indicated previously, the lower limit for the radial variable r' in V_2 was 0 and the contribution from V_1 was neglected completely. The volume integrations over V_2 were carried out analytically, however the various integrations with respect to ζ were determined numerically for various values of s. The general form found for F_L is

$$F_L = \kappa^2 Re\,[\beta'^2 G_1(s) + \beta'\gamma' G_2(s)], \tag{5.24}$$

with the convention that a positive force is in the direction of increasing s while a negative force is in the opposite direction. The functions $G_1(s)$ and $G_2(s)$, which are independent of the detailed undisturbed flow, were evaluated numerically for various values of s and are listed in table 4. It is found that

$$G_1(s) = -G_1(1-s), \quad G_2(s) = G_2(1-s), \tag{5.25}$$

and $G_1(s)$ is positive for $0 < s < 0{\cdot}5$ whereas $G_2(s)$ is always positive. The general expression (5.24) for the lateral force is applicable to all undisturbed flow fields of the form $\alpha + \beta' z' + \gamma' z'^2$.

A careful examination of (5.24) indicates the following general behaviour of the individual terms. The first term, which is the interaction of the disturbance stresslet and its wall correction with the bulk shear (hence proportional to β^2), in all cases produces an inward force which tends to cause migration toward the centre-line $s = 0{\cdot}5$. The second term, which is the interaction between the Stresslet and the curvature of the bulk velocity profile (hence proportional to $\beta\gamma$), tends to cause migration in the direction of increasing (absolute) shear rate. For every example of two-dimensional shear flow $\alpha + \beta' z' + \gamma' z'^2$ involving either moving walls, an imposed pressure gradient or a combination of these, the region of largest shear is near one (or both) of the walls.

Reverting to dimensional variables and substituting for $\beta' = V_w = 2V_m$ and $\gamma' = 0$ in (5.24), the lateral force for simple shear flow is thus

$$F_L^* = \rho_0 V_m^{*2} a^2 \kappa^2 [4G_1(s)], \tag{5.26}$$

which is plotted in figure 2. Hence, for this case, the lateral force is in the positive-z direction for $0 < s < 0{\cdot}5$ and in the negative-z direction for $0{\cdot}5 < s < 1{\cdot}0$. Thus, a stable equilibrium position for the sphere in a simple shear flow between two

s	G_1	G_2	s	G_1	G_2
0·50	0·0	1·072	0·25	0·885	0·711
0·49	0·0419	1·070	0·24	0·907	0·683
0·48	0·0837	1·068	0·23	0·927	0·654
0·47	0·1254	1·066	0·22	0·945	0·625
0·46	0·1669	1·062	0·21	0·960	0·596
0·45	0·2080	1·056	0·20	0·973	0·566
0·44	0·2489	1·050	0·19	0·982	0·536
0·43	0·2894	1·042	0·18	0·988	0·506
0·42	0·3293	1·033	0·17	0·990	0·477
0·41	0·3688	1·023	0·16	0·988	0·448
0·40	0·4077	1·012	0·15	0·981	0·420
0·39	0·4459	1·000	0·14	0·971	0·393
0·38	0·4834	0·987	0·13	0·957	0·368
0·37	0·520	0·972	0·12	0·943	0·345
0·36	0·556	0·956	0·11	0·931	0·324
0·35	0·591	0·940	0·10	0·927	0·306
0·34	0·626	0·922	0·09	0·940	0·292
0·33	0·659	0·902	0·08	0·982	0·282
0·32	0·691	0·882	0·07	1·07	0·278
0·31	0·723	0·861	0·06	1·23	0·280
0·30	0·753	0·838	0·05	1·50	0·291
0·29	0·782	0·815	0·04	1·93	0·315
0·28	0·810	0·790	0·03	2·58	0·354
0·27	0·836	0·765	0·02	3·59	0·414
0·26	0·861	0·738	0·01	5·33	0·505

TABLE 4. Values of G_1 and G_2; $G_1(s) = -G_1(1-s)$, $G_2(s) = G_2(1-s)$.

plane walls is the centre-line $s = 0{\cdot}5$, where $G_1(s) = 0$. This value agrees reasonably well with the experimental observations of Halow & Wills (1970*a*, *b*), who found a stable equilibrium position between $s = 0{\cdot}5$ and 0·55 in a concentric-cylinder Couette flow. In the next section, we shall show that the slight apparent discrepancy in these two results is due to the curvature of the Couette flow streamlines.

For the case of two-dimensional Poiseuille flow, where $\beta' = 4V_{\max}(1-2s)$ and $\gamma' = -4V_{\max}$, the dimensional expression for the lateral force is

$$F_L^* = \rho_0 V_m^{*2} a^2 \kappa^2 [36(1-2s)^2 G_1(s) - 36(1-2s) G_2(s)], \tag{5.27}$$

which is also plotted in figure 2. Clearly the portion $\beta'^2 G_1(s)$ of the force which involves the square of the shear rate tends to push the sphere to the centre, while the term $\beta'\gamma' G_2(s)$, which involves the product of the shear rate and its rate of change, is negative for $0 < s < 0{\cdot}5$ and the positive for $0{\cdot}5 < s < 1$, thus opposing the effect of the first term. There are three positions where the force F_L is zero: the centre-line ($s = 0{\cdot}5$), which is unstable to slight perturbations, and $s = 0{\cdot}2$ and 0·8, which are stable equilibrium points. Unfortunately, the only available experiments for two-dimensional Poiseuille flow, those of Repetti & Leonard (1966) and of Tachibana (1973), are somewhat inconclusive with regard

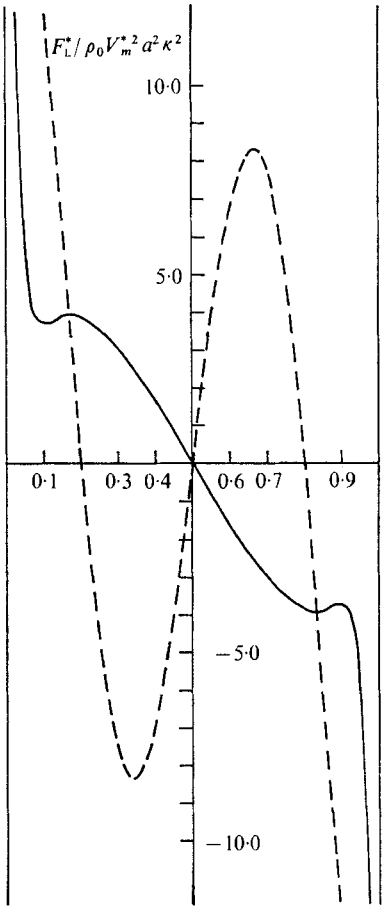

FIGURE 2. Lateral force $F_L^*/\rho_0 V_m^* a^2\kappa^2$ as a function of lateral position. ——, simple shear flow; – – –, two-dimensional Poiseuille flow.

to the equilibrium position. In Repetti & Leonard's experiments, the particles were never quite neutrally buoyant. Rewriting the criterion (5.23), we require

$$|\rho_s - \rho_0| \ll \mu_0 V_m^*/d^2 g.$$

Using the maximum viscosity and velocity estimates of 10 cP and 2 cm/s, $\mu_0 V_m^*/d^2 g \sim 10^{-5}$ for Repetti & Leonard's experimental set-up. On the other hand, the density differences were never measured more accurately than to within $\pm 10^{-4}$. The fact that the particles were never really neutrally buoyant may explain why Repetti & Leonard were unable to obtain reliable and conclusive results for the equilibrium position with their 'neutrally buoyant' spheres. The equilibrium positions reported by Tachibana (1973) also exhibit a great deal of scatter. However, Tachibana presented sphere trajectories only for two cases with equilibrium positions of $s = 0{\cdot}2$ and $0{\cdot}8$, which, for reasons that are not clear from his paper, he apparently felt to be the most reliable.

These equilibrium values agree perfectly with the present theoretical predictions.

Finally, it is interesting to note that the predicted equilibrium positions for two-dimensional Poiseuille flow are precisely equivalent to the value measured in a *circular* tube by Segré & Silberberg (1962*a*, *b*). In addition, the form (5.27) for F_L^* in this case is essentially the same as Segré & Silberberg's empirical estimate (cf. the discussion by Brenner 1966, p. 381).

6. Particle trajectories

It is of interest to use the result for the force to calculate the trajectories of the sphere. In particular, the calculated sphere trajectories can be compared with available experimental results reported in the literature. The lateral velocity has been found to be given in dimensional form by

$$Re\, U_{sz}^{(1)*} = \frac{F_L^*}{6\pi\mu_0 a} = \frac{\rho_0 V_m^{2*} d}{6\pi\mu_0}\kappa^3 G(s), \tag{6.1}$$

in which $G(s)$ is given by $$G(s) = 4G_1(s) \tag{6.2a}$$

for simple shear flow and by

$$G(s) = 36[(1-2s)^2 G_1(s) - (1-2s)\, G_2(s)] \tag{6.2b}$$

for two-dimensional Poiseuille flow. The sphere trajectories can be expressed in terms of the lateral position of the particle either as a function of time or as a function of axial position in the flow channel. Since the lateral velocity $U_{sz}^{(1)*}$ can be expressed as

$$Re\, U_{sz}^{(1)*} = d\frac{ds}{dt^*} = \frac{\rho_0 V_m^{*2} d}{6\pi\mu_0}\kappa^3 G(s) \tag{6.3}$$

and the axial velocity as

$$U_{sx}^{(0)*} = d\, dx'/dt^* = \alpha + O(\kappa^2), \tag{6.4}$$

the trajectory equation may be expressed either as

$$dt^* = \frac{6\pi\mu_0}{\rho_0 V_m^{*2}\kappa^3 G(s)}\, ds \tag{6.5}$$

or equivalently

$$dx' = \frac{6\pi\mu_0\alpha}{\rho_0 V_m^{*2} d\kappa^3 G(s)}\, ds. \tag{6.6}$$

For the time trajectory, we have for both simple shear and two-dimensional Poiseuille flow

$$t^* - t_0^* = \frac{6\pi\mu_0}{\rho_0 V_m^{*2}\kappa^3}\int_{s_0}^{s}\frac{ds'}{G(s')}, \tag{6.7}$$

and for the axial-position trajectory in the simple shear flow case

$$(\alpha = V_w^* s = 2V_m^* s),$$

we have

$$x' - x_0' = \frac{12\pi\mu_0}{\rho_0 V_m^* d\kappa^3}\int_{s_0}^{s}\frac{s'\, ds'}{G(s')}, \tag{6.8}$$

while in the two-dimensional Poiseuille flow case

$$(\alpha = 4V_{\max}^* s(1-s) = 6V_m^* s(1-s)),$$

$$x' - x_0' = \frac{36\pi\mu_0}{\rho_0 V_m^* d\kappa^3}\int_{s_0}^{s}\frac{s'(1-s')}{G(s')}\, ds'. \tag{6.9}$$

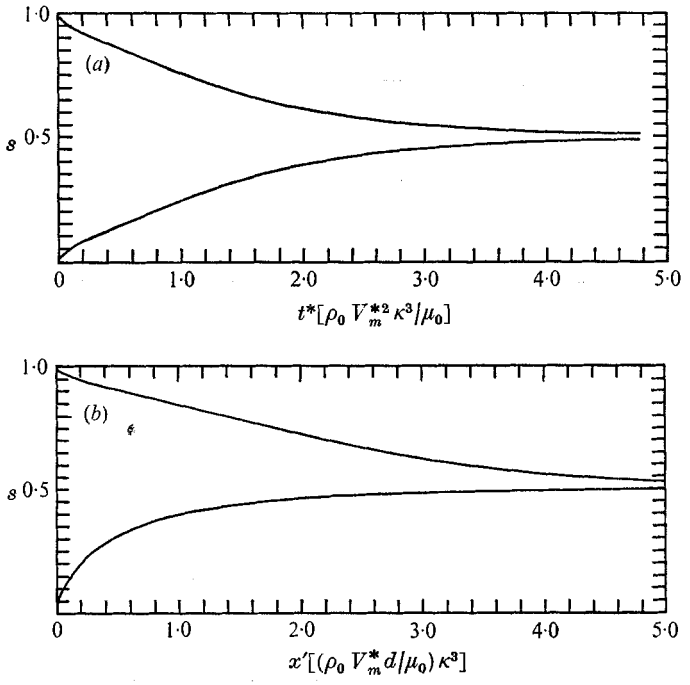

FIGURE 3. Particle trajectory for simple shear flow: lateral position *vs.* (*a*) time and (*b*) axial position.

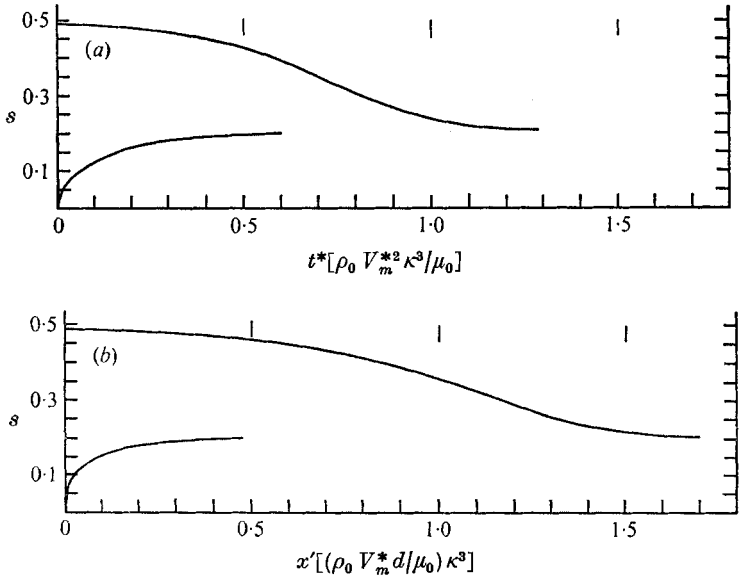

FIGURE 4. Particle trajectory for two-dimensional Poiseuille flow: lateral position *vs.* (*a*) time and (*b*) axial position.

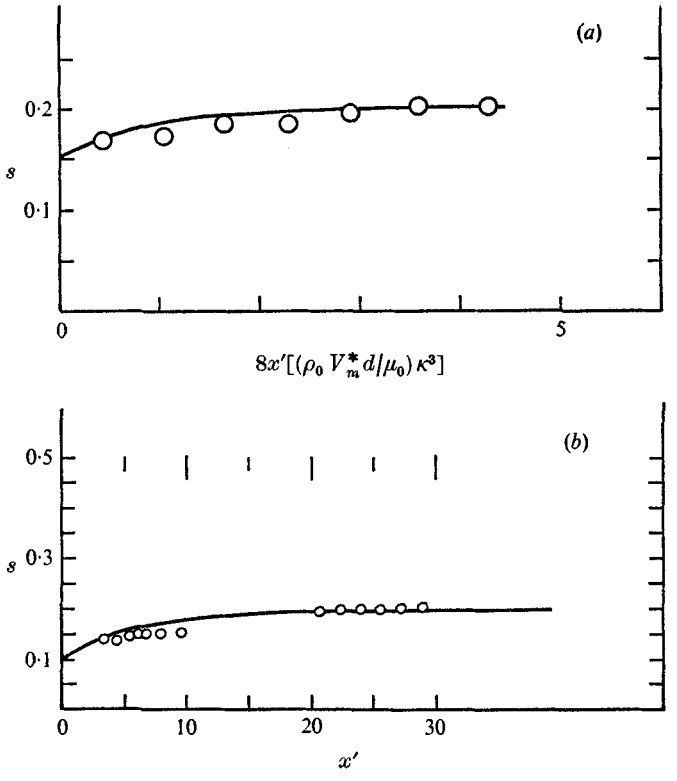

FIGURE 5. A comparison of experimental particle trajectories (Tachibana) in two-dimensional Poiseuille flow with the present theory: ○, experimental (Tachibana); ——, present theory. In (*a*), the lateral position s is plotted *vs.* $8x'[(\rho_0 V_m^* d/\mu_0)\kappa^3]$; and in (*b*) the lateral position s is plotted *vs.* x' with $\rho_0 V_m d/\mu_0 = 32{\cdot}1$ and $\kappa = 0{\cdot}0795$.

For simple shear flow, the particle trajectories (6.7) and (6.8) are plotted in figures 3(*a*) and (*b*) with s_0 taken to be 0·01 and 0·99. The time trajectory is symmetric about $s = 0{\cdot}5$ while the axial-position trajectory is not. For two-dimensional Poiseuille flow, (6.7) and (6.9) are plotted in figures 4(*a*) and (*b*). Since in this case both time and axial-position trajectories are symmetric about $s = 0{\cdot}5$, only $s_0 = 0{\cdot}01$ and 0·49 are considered. The main feature of interest for Poiseuille flow, which we shall discuss at greater length in the following section, is the skewness of the trajectories in the sense that spheres near the wall clearly migrate more rapidly than those near the centre for a given average flow rate V_m^* in a given fluid. This feature reflects the larger lateral force associated with the region nearest the wall.

For the reasons discussed in the previous section, the trajectories of Repetti & Leonard (1966) cannot be compared with our present theory. The only available experimental results are those of Tachibana (1973) and Halow & Wills (1970*a*, *b*).

Tachibana (1973) studied the migration of neutrally buoyant rigid spheres in two- and three-dimensional Poiseuille flow. Particle trajectories giving lateral *vs.* axial position were measured for the two cases cited earlier in which the equilibrium positions were $s = 0{\cdot}2$ and $s = 0{\cdot}8$. These trajectories are reproduced in

figures 5(*a*) and (*b*) together with corresponding trajectories predicted by the present theory. The agreement between observation and theory is remarkably good.

Halow & Wills' experimental investigation of sphere migration was carried out in a Couette flow system in which the inner cylinder was rotated and the outer cylinder was held fixed. For gap widths small compared with the cylinder radius the flow may be approximated as a simple shear flow. Extensive results are given in the thesis of Halow (1968) and our comparison is drawn from this source. As we have indicated earlier, Halow (1968) found the equilibrium position to be close to the centre-line between the two walls, but also somewhat closer to the inner moving wall, corresponding to a value of s between 0·5 and 0·55 in our present nomenclature. We believe that the slight discrepancy between these values and the predicted value of 0·5 is due to the fact that the Couette flow in Halow's apparatus corresponds only approximately to a simple shear flow. In fact, the ratio $2d/(r_1+r_2)$ has values of 0·1, 0·17, 0·22 and 0·3 in his experiments, where r_1 and r_2 are the inner and outer cylinder radii. The case corresponding to the value 0·1 is the nearest to simple shear flow, however, in this case the shear rates are too large to be compared with the present small-inertia expansion. The case 0·17 has sufficiently small shear rates; however, the flow is slightly different from a simple shearing flow.

In order to provide a detailed comparison with the data of Halow (1968), we therefore modify the analysis which is presented in the previous sections for simple shear flow to include the effects of curvature in the velocity distribution. Hence, instead of assuming simple shear flow, let us write an exact expression for the tangential undisturbed velocity field with co-ordinate axes fixed at the centre of the particle:

$$V^* = V_w^* \left(s+\frac{z^*}{d}\right)\left[\frac{r_1(r_2+r)}{r(r_2+r_1)}\right]. \tag{6.10}$$

Here, V_w^* is the tangential velocity of the inner wall, s is the non-dimensional lateral position of the sphere measured from the outer wall, z^* is the lateral position measured from the sphere centre and r (dimensional) is the radial position measured from the centre of the coaxial cylinders. Thus, the factor $r_1(r_2+r)/r(r_2+r_1)$ provides a correction of the simple shear flow profile for the Couette geometry. Provided that $2d/(r_1+r_2)$ is small, we can write

$$\frac{r_1(r_2+r)}{r(r_2+r_1)} = 1-\frac{r_2(r_2-r_1)}{r_1(r_2+r_1)}\left(1-s-\frac{z^*}{d}\right) \tag{6.11}$$

or

$$\begin{aligned} V^* &= V_w^*\left(s+\frac{z^*}{d}\right)\left[1-\frac{r_2(r_2-r_1)}{r_1(r_2+r_1)}(1-s)+\frac{r_2(r_2-r_1)z^*}{r_1(r_2+r_1)d}\right] \\ &= V_m^* s\left[1-\frac{r_2(r_2-r_1)}{r_1(r_2+r_1)}(1-s)\right]+V_w^*\left[1-\frac{r_2(r_2-r_1)}{r_1(r_2+r_1)}(1-2s)\right]\frac{z^*}{d} \\ &\quad + V_w^*\left[\frac{r_2(r_2-r_1)}{r_1(r_2+r_1)}\right]\left(\frac{z^*}{d}\right)^2. \end{aligned} \tag{6.12}$$

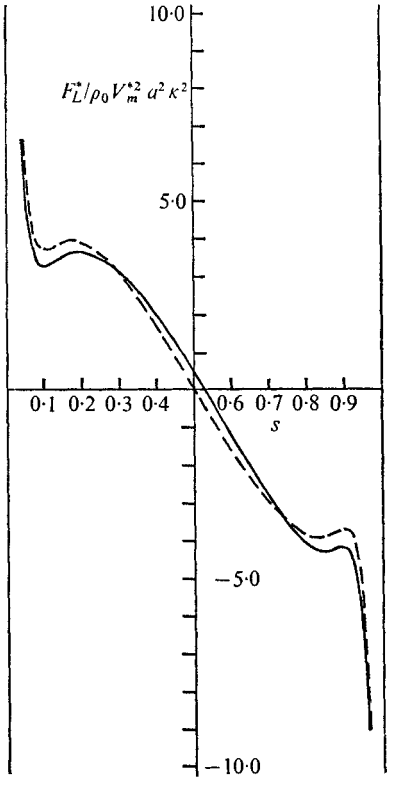

FIGURE 6. A comparison of the lateral force for simple shear flow with that for Couette flow. – – –, simple shear flow; ——, Couette flow with $R = 0{\cdot}1$.

The deviation of the Couette flow profile from simple shear flow depends on the parameter $R = r_2(r_2 - r_1)/r_1(r_2 + r_1)$. We can express the tangential velocity in dimensionless form as

$$V = \alpha + \beta' z' + \gamma' z'^2,$$

where

$$\alpha = V_w s[1 - R(1-s)], \quad \beta' = V_w[1 - R(1-2s)], \quad \gamma' = V_w R. \quad (6.13a, b, c)$$

Hence, our general result (5.24) can be used to calculate the force

$$F_L = Re\,\kappa^2[\beta'^2 G_1(s) + \beta'\gamma' G_2(s)].$$

We have plotted the result for the force with the parameter $R = 0{\cdot}1$ (corresponding to the case of $2d/(r_1 + r_2) = 0{\cdot}17$) in figure 6. Also shown is the force for simple shearing flow. The equilibrium position is seen to be shifted to $s = 0{\cdot}53$. The corresponding sphere trajectory, in the form of lateral position *vs.* time, is plotted in figure 7. On the same figure are the experimental results of Halow (1968) for the corresponding case in which the gap width d is 9·48 mm and $R = 0{\cdot}101$. Again reasonable agreement between theory and experiment is found.

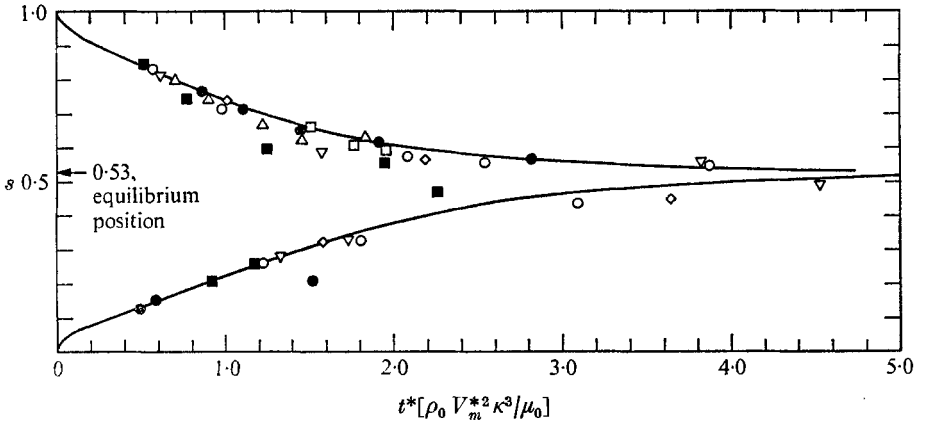

FIGURE 7. A comparison of experimental particle trajectories (Halow) in Couette flow with the present theory (solid line). In the results of Halow, d = 9·48 mm, r_2 = 60 mm, r_1 = 51 mm and R = 0·101. The following points and numbers correspond to different sphere radii reported in the thesis of Halow: ◇, 5, 6 (a = 0·8495 mm); ○, 11, 12 (a = 0·8495 mm); ■, 15, 16 (a = 0·636 mm); △, 19 (a = 0·735 mm); □, 20 (a = 0·537 mm); ▽, 25, 26 (a = 0·296 mm); ●, 27, 28 (a = 0·296 mm).

7. Flow of a suspension of rigid spherical particles which undergo translational Brownian motion

As a specific application of the results of the preceding sections, we consider the motion of a dilute suspension of rigid spheres which are simultaneously undergoing inertia-induced lateral migration and translational Brownian motion.

Of course, the preceding results have been derived for a *single* sphere in a given bulk flow, and it is necessary to investigate the circumstances in which the lateral force calculated for that case is applicable to a particle in a suspension of many particles. We have seen that the role of the walls is critical in the migration phenomenon and acts essentially by modifying the inertial behaviour of the flow. In addition, the walls also cause the sphere to have translational and rotational velocities different from those of the surrounding fluid, but the lateral force induced by this difference is smaller by $O(\kappa)$. If we now consider *two* spheres present in the bulk flow, it is clear that the modification of the inertial behaviour of the fluid would not be changed significantly from the single-sphere case because the second sphere constitutes the addition, in effect, of a boundary infinitesimally small compared with the infinitely unbounded walls. In addition, each sphere would also translate and rotate in creeping motion at different velocities as compared with a single sphere. This difference is of order $(a/d)\,(a/l)^2$ for translational motion and $(a/d)\,(a/l)^3$ for rotational motion, l being the inter-particle distance (see Wakiya, Darabaner & Mason 1967; Batchelor & Green 1972). However, we have previously shown that the lateral force will not be affected unless the translational and angular velocities of the sphere are changed to order $(a/d)^2$ and a/d respectively [cf. (5.15)]. Hence, the conditions for neglecting two-particle *inertial* migration compared with the single-particle/wall migration are

$$(a/l)^2 \ll a/d, \quad (a/l)^3 \ll 1. \tag{7.1a, b}$$

For a dilute suspension of concentration Φ ($\sim a^3/l^3$), the condition (7.1*b*) is automatically satisfied and (7.1*a*) becomes

$$\Phi^2 \ll \kappa^3. \tag{7.2}$$

In addition to two-particle inertial migration, it is *possible* that three-particle interactions may cause migration even at *zero* Reynolds number since the collision process is not reversible. Since three-particle interactions have a probability of occurrence $O(\Phi^2)$, a *conservative* condition for the neglect of this effect relative to wall-induced single-particle inertial migration is $\Phi^2 \ll \kappa^2 Re$, or since $Re \ll \kappa^2$,

$$\Phi^2 \ll \kappa^4. \tag{7.3}$$

Hence, if the conditions (7.2) and/or (7.3) are satisfied, it may be assumed that the lateral force on a particle in a suspension is equal to that on a single sphere immersed in the fluid.

Here, we consider the concentration distributions, flow behaviour and effective viscosity of a suspension of uniformly sized rigid spheres undergoing lateral migration with simultaneous Brownian translation in simple shear flow and two-dimensional Poiseuille flow. The concentration distribution is established as the result of a competition between the lateral migration force, which tends to cause the particles to crowd to a preferred position, and Brownian motion, which tends to cause a uniform dispersion across the channel. For our present purposes, we consider only the simple situation of *steady* bulk flow in which the concentration distribution has achieved its final, steady-state configuration.

The governing equation for the steady-state probability density function $\Phi(s)$ for concentration can be written as

$$d[\Phi(U^*_{\mathrm{Br}} + Re\, U^*_{sz})]/ds = 0. \tag{7.4}$$

Here U^*_{Br} represents the effective lateral velocity due to the action of Brownian diffusion in the presence of a concentration gradient, i.e.

$$\Phi U^*_{\mathrm{Br}} = -\left(\frac{kT}{6\pi\mu_0 a}\right)\frac{1}{d}\frac{d\Phi}{ds}, \tag{7.5}$$

where $kT/6\pi\mu_0 a$ is the translational Brownian diffusion coefficient, with k as the Boltzmann constant and T the absolute temperature. The velocity in the z direction induced by inertia is

$$Re\, U^*_{sz} = F^*_L(s)/6\pi\mu_0 a. \tag{7.6}$$

It should be noted that each of (7.5) and (7.6) is only a first approximation in κ. The solution of (7.4) with (7.5) and (7.6) is simply

$$\Phi(s) = \Phi_m \exp\left[\frac{d}{kT}\int_{\frac{1}{2}}^{s} F^*_L(s')\,ds'\right] \Big/ \int_{s=0}^{1} \exp\left[\frac{d}{kT}\int_{\frac{1}{2}}^{s''} F^*_L(s')\,ds'\right] ds'', \tag{7.7}$$

where Φ_m is the mean concentration

$$\Phi_m \equiv \int_0^1 \Phi(s')\,ds'$$

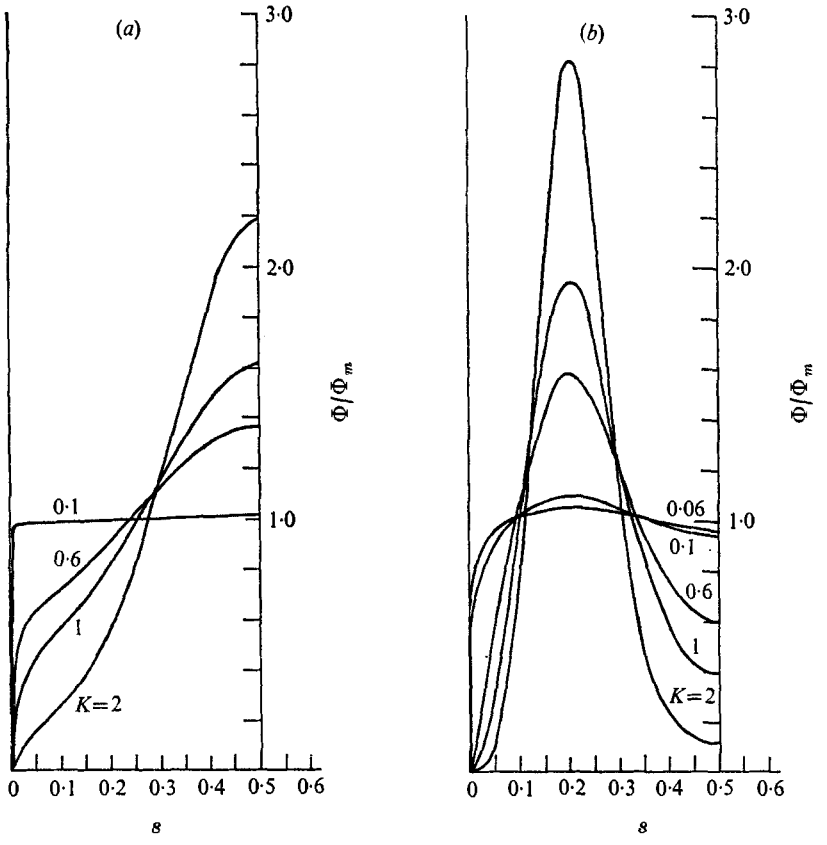

FIGURE 8. Concentration distribution $\Phi(s)/\Phi_m$ for various K in (*a*) simple shear flow and (*b*) two-dimensional Poiseuille flow.

and the lower limit of the integral of $F_L^*(s')$ is taken to be $\frac{1}{2}$ for convenience. Substituting the general form for F_L^*, i.e.

$$F_L^*(s) = \rho_0 V_m^{*2} a^2 \kappa^2 G(s),$$

and defining the parameter $K = \rho_0 V_m^{*2} a^4/dkT$, the concentration distribution function may thus be expressed as

$$\Phi(s) = \Phi_m \exp\left[K\int_{\frac{1}{2}}^{s} G(s')\,ds'\right] \Big/ \int_{s''=0}^{1} \exp\left[K\int_{\frac{1}{2}}^{s''} G(s')\,ds'\right] ds''. \tag{7.8}$$

The function $\Phi(s)$ is plotted with K as a parameter in figures 8(*a*) and (*b*). Since the distributions are symmetric about $s = 0{\cdot}5$, only half of the channel width is considered. Clearly $K \sim 10$ is inertia controlled whereas $K \sim 0{\cdot}01$ is diffusion controlled, these cases corresponding, respectively, to sharply peaked and nearly uniform concentration distributions.

Provided that (7.2) and/or (7.3) are satisfied *even at the most concentrated region*, the local effective viscosity at any position s may be calculated using the classical formula of Einstein

$$\mu(s) = \mu_0[1 + \tfrac{5}{2}\Phi(s)]. \tag{7.9}$$

There is an additional correction term due to the presence of inertia. For example, in an unbounded system, Lin, Peery & Schowalter (1970) have shown that the correction is $O(Re^{\frac{3}{2}})$. For small Reynolds number, we can neglect this correction and consider only the correction due to a non-uniform particle distribution. Since Φ depends upon s, so does μ, and the velocity profiles for the suspension as a whole will differ slightly (by $O(\Phi_m)$) from their simple form for a fluid of constant viscosity. This change may then be reflected in the relationship between the pressure drop and flow rate ($\Delta P/L$ versus Q) for the Poiseuille flow, and in the relationship between the applied force F_w^* and wall velocity V_w^* for simple shear flow. Hence, an investigator measuring $\Delta P/L$ and Q, or F_L^* and V_w^* as a viscometric measurement for an assumed purely viscous fluid of uniform viscosity would be led to conclude the existence of non-Newtonian behaviour since $\Phi(s)$ changes as a function of the flow rate. The equations for a steady-state unidirectional velocity field in the case of spatially varying local viscosity are simply

$$\frac{d}{ds}\left[\mu(s)\frac{du}{ds}\right] = 0; \quad u = 0 \quad \text{at} \quad s = 0; \quad u = V_w^* \quad \text{at} \quad s = 1, \tag{7.10}$$

for simple shear flow, and

$$\frac{d}{ds}\left[\mu(s)\frac{du}{ds}\right] = \left(\frac{\Delta P}{L}\right)d^2; \quad u = 0 \quad \text{on} \quad \text{the walls}, \tag{7.11}$$

for two-dimensional Poiseuille flow. By solving these equations, the modified velocity profiles can be shown to be

$$\frac{u(s)}{V_w^*} = s + \frac{5}{2}\left[s\Phi_m - \int_0^s \Phi(s')\,ds'\right] \tag{7.12}$$

for simple shear flow and

$$\frac{u(s)}{\frac{3}{2}V_m^*} = [1-(1-2s)^2] + \frac{5}{2}\left\{3[1-(1-2s)^2]\int_0^1 (1-2s')^2\,\Phi(s')\,ds' - 4\int_0^s (1-2s')\,\Phi(s')\,ds'\right\} \tag{7.13}$$

for two-dimensional Poiseuille flow. If $\Phi(s) = \Phi_m$, these expressions reduce to

$$u(s)/V_w^* = s, \tag{7.14}$$

$$u(s)/\tfrac{3}{2}V_m^* = 1-(1-2s)^2, \tag{7.15}$$

which are the appropriate velocity profiles for a fluid of constant viscosity. For simple shear flow, the correction term, (7.14) subtracted from (7.12),

$$\frac{5}{2}\left[s\Phi_m - \int_0^s \Phi(s')\,ds'\right] \tag{7.16}$$

is positive for $0 < s < 0{\cdot}5$ and negative for $0{\cdot}5 < s < 1$, and it is odd about $s = 0{\cdot}5$. Thus, from (7.12), the suspension moves more rapidly near the fixed wall and more slowly near the moving wall as compared with (7.14). For two-dimensional Poiseuille flow, the correction term, (7.15) subtracted from (7.13),

$$\frac{5}{2}\left\{3[1-(1-2s)^2]\int_0^1 (1-2s')^2\,\Phi(s')\,ds' - 4\int_0^s (1-2s')\,\Phi(s')\,ds'\right\} \tag{7.17}$$

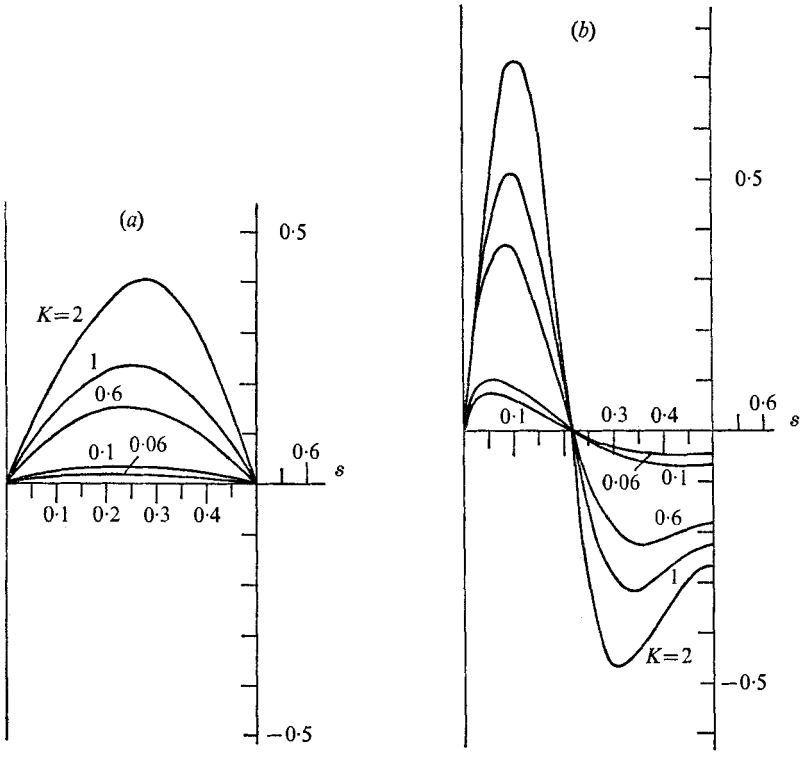

FIGURE 9. Correction term in velocity profile for (*a*) simple shear flow, equation (7.16), and (*b*) two-dimensional Poiseuille flow, equation (7.17).

is negative for $0{\cdot}22 < s < 0{\cdot}78$ and positive for $0 < s < 0{\cdot}22$ and $0{\cdot}78 < s < 1$, and is even about $s = 0{\cdot}5$. Thus, the resulting motion (7.13) is more rapid near the walls and slower near the centre as compared with (7.15). These correction terms (7.16) and (7.17) are plotted in figures 9(*a*) and (*b*) for various values of K. We have also plotted the resulting velocity profiles corresponding to (7.12) and (7.13) in figures 10(*a*) and (*b*) for $K = 2$ and $\Phi_m = 0{\cdot}1$. Although the present small-Φ theory is not expected to hold at a value of Φ_m as large as this, this value does allow the predicted corrections to be discernible on the scale of the bulk flow field. The most interesting feature evident in this figure is the flattening of the velocity profile for the case of two-dimensional Poiseuille flow.

It is of greatest interest to calculate the apparent viscosity μ_{app}, which would be measured by interpretating force/wall velocity or pressure drop/flow rate data as though the particle concentration was uniform, and the suspension therefore Newtonian with a constant viscosity. For simple shear flow, this apparent viscosity may be expressed as

$$\mu_{\text{app}} = F_w^* d / V_w^*, \tag{7.18}$$

where F_w^* is the applied force (equal also to the force required to keep the stationary wall fixed) and V_w^* the velocity of the moving wall. Similarly, for a two-dimensional Poiseuille flow, the apparent viscosity is

$$\mu_{\text{app}} = -\tfrac{1}{12}(\Delta P/L)\, d^3/Q, \tag{7.19}$$

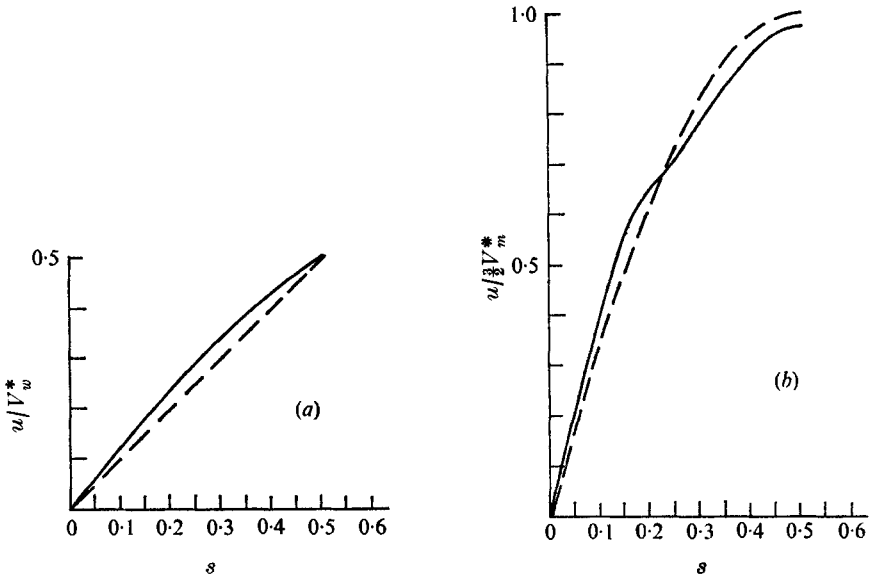

FIGURE 10. Velocity profile for (*a*) simple shear flow and (*b*) two-dimensional Poiseuille flow. – – –, uniform particle distribution; ——, non-uniform particle distribution with $K = 2$, $\Phi = 0{\cdot}1$.

where $\Delta P/L$ and Q are the measured pressure gradient and volumetric flow rate. Using the velocity profiles (7.12) and (7.13), plus the expression (7.9) for the effective *local* viscosity, we evaluate (7.18) and (7.19) to obtain the results

$$\mu_{\text{app}} = \mu_0[1 + \tfrac{5}{2}\Phi_m + O(\Phi_m^2)] \tag{7.20}$$

for simple shear flow and

$$\mu_{\text{app}} = \mu_0\left[1 + \frac{5}{2}\int_0^1 3\Phi(s')\,(1-2s')^2\,ds' + O(\Phi_m^2)\right] \tag{7.21}$$

for two-dimensional Poiseuille flow. Thus the apparent effective viscosity will be independent of the flow rate (shear rate) and equal to the Einstein value with Φ replaced by Φ_m for simple shear flow, but distinctly flow-rate dependent ('non-Newtonian') for two-dimensional Poiseuille flow. We have plotted the expression (7.21) for μ_{app} as a function of the flow-rate parameter K in figure 11. The deviation from the simple Newtonian value corresponding to a uniform concentration distribution ($K = 0$) first decreases with K but then for $K > \sim 0{\cdot}5$ increases monotonically towards the approximate asymptotic value

$$(\mu_{\text{app}} - \mu_0)/\mu_0 = \tfrac{5}{2}\Phi_m(1{\cdot}06).$$

Although this behaviour may appear unusual and at variance with the available data of Segré & Silberberg (1963), it is easily understood on the basis of the present theory. In a non-uniform shear flow, the contribution which a given particle makes to the dissipation of energy (and hence to the effective viscosity) depends on the square of the local velocity gradient. A particle near the wall, for example, contributes a greater fraction of the overall rate of dissipation

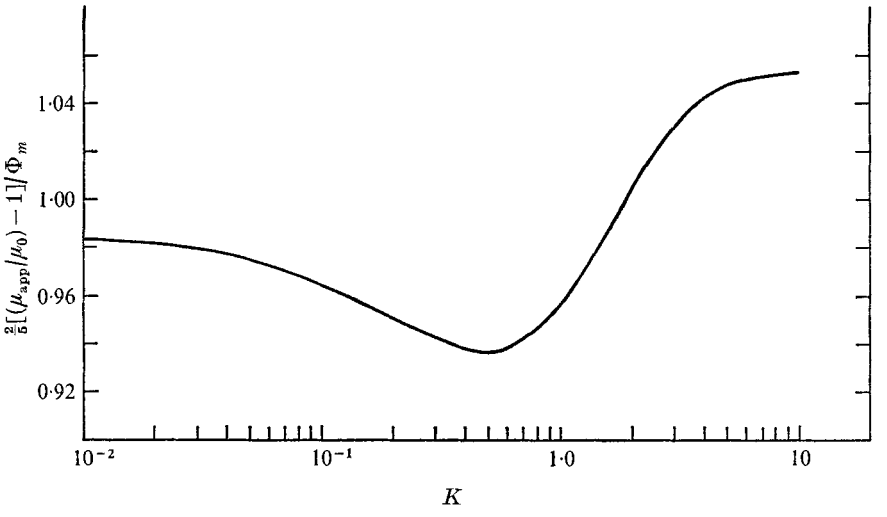

FIGURE 11. Reduced viscosity $\frac{2}{5}(\mu_{app}/\mu_0 - 1)/\Phi_m$ *vs.* K for two-dimensional Poiseuille flow.

than does a particle which is near to the centre-line, where the local shear rate is small. In addition, we have seen (cf. figure 2) that the lateral force is greatest near the wall and least near the centre-line. Hence, as K is increased, the migration of particles from the wall towards the 'equilibrium' position is more effective than the migration from the region nearer the centre-line, and the steady-state concentration distribution becomes skewed in favour of more particles in the centre and less near the walls (cf. figure 8*b*). Thus, initially the change in μ_{app} is towards lower values as the decrease in dissipation due to migration away from the walls dominates the increase caused by outward migration from the vicinity of the centre-line. For some intermediate value of K, the effective viscosity begins to increase as the outward migration from the centre becomes comparable with the inward migration from the walls. The data of Segré & Silberberg (1963) show only a decrease in viscosity with increasing flow rate. However, owing to the large particles used ($a = 0{\cdot}6$ mm), the values of K ($\sim 10^8$) are well into the migration-dominated regime where Φ is not small near the equilibrium position and particle–particle interactions are important.

This work was supported, in part, by grant 6489-AC7 from the Petroleum Research Fund, administered by the American Chemical Society, and, in part, by NSF grant GK-35468.

REFERENCES

BATCHELOR, G. K. & GREEN, J. T. 1972 *J. Fluid Mech.* **56**, 375.
BRENNER, H. 1966 *Advances in Chemical Engineering*, vol. 4. Academic.
BRETHERTON, F. P. 1962 *J. Fluid Mech.* **14**, 284.
COX, R. G. & BRENNER, H. 1968 *Chem. Engng Sci.* **23**, 147.

GOLDSMITH, H. L. & MASON, S. G. 1966 *Rheology: Theory and Applications* (ed. F. R. Eirich), vol. 4. Academic.

HALOW, J. S. 1968 Ph.D. thesis, Virginia Polytechnic Institute.

HALOW, J. S. & WILLS, G. B. 1970*a* *A.I.Ch.E. J.* **16**, 281.

HALOW, J. S. & WILLS, G. B. 1970*b* *Ind. Eng. Chem. Fund.* **9**, 603.

HAPPEL, J. & BRENNER, H. 1973 *Low Reynolds Number Hydrodynamics.* Noordhoff.

HO, B. P. 1974 Ph.D. thesis, California Institute of Technology.

LIN, C. J., PEERY, J. H. & SCHOWALTER, W. R. 1970 *J. Fluid Mech.* **44**, 1.

REPETTI, R. V. & LEONARD, E. F. 1966 *Chem. Engng Prog. Symp. Ser.* **62**, 80.

RUBINOW, S. I. & KELLER, J. B. 1961 *J. Fluid Mech.* **11**, 447.

SAFFMAN, P. G. 1965 *J. Fluid Mech.* **22**, 385.

SEGRÉ, G. & SILBERBERG, A. 1962*a* *J. Fluid Mech.* **14**, 115.

SEGRÉ, G. & SILBERBERG, A. 1962*b* *J. Fluid Mech.* **14**, 136.

SEGRÉ, G. & SILBERBERG, A. 1963 *J. Colloid Sci.* **18**, 312.

STARKEY, T. V. 1956 *Brit. J. Appl. Phys.* **7**, 52.

TACHIBANA, M. 1973 *Rheol. Acta*, **12**, 58.

WAKIYA, S. J. 1956 *Res. Rep. Fac. Engng, Niigata University (Japan)*, **5**, 1.

WAKIYA, S., DARABANER, C. L. & MASON, S. G. 1967 *Rheol. Acta*, **6**, 264.